The Two Centre Dirac Equation *

Berndt Müller and Walter Greiner

Institut für Theoretische Physik der Johann Wolfgang Goethe-Universität,
Frankfurt am Main, Germany
and
Wright Nuclear Structure Laboratory, Yale University, New Haven, Connecticut, USA

During collisions of heavy ions with heavy targets below the Coulomb barrier, adiabatic molecular orbitals are formed for the inner electrons. Deviations from adiabaticity lead to coupling between various states and can be treated by time-dependent perturbation theory. For high charges $(Z_1 + Z_2 \geq 60)$ the molecular electrons are highly relativistic. Therefore, the Dirac equation has to be used to obtain the energies and wave functions. The Dirac Hamiltonian is transformed into the intrinsic rotating coordinate system where prolate spheroidal coordinates are introduced. A set of basis functions is proposed which allows the evaluation of all matrix elements of the Dirac Hamiltonian analytically. The resulting matrix is diagonalized numerically. The finite nuclear charge distribution is also taken into account. Results are presented and discussed for various characteristic systems, e. g. Br—Br, Ni—Ni, I—I, Br—Zr, I—Au, U—U, etc.

I. Introduction

The formation of molecular electronic states for inner electrons in light ion collisions was first recognized and interpreted as such by Fano and Lichten [1] in connection with the so-called promotion model for ionization. This was applied to account for large ionization cross sections of certain electronic states during a collision that could not be accounted for by pure Coulomb ionization. The promotion mechanism was later extended to asymmetric collisions by Barat and Lichten [2], and a theoretical justification of the diabatic molecular states was given by Smith [3] (see, however, the paper of Gabriel and Taulbjerg [3]).

Independently, and stimulated by the nuclear molecular phenomena [4a] and by the nuclear two center shell model [4b], the idea of intermediate electronic molecular states formed in the collision of heavy ions was put forward in connection with possible tests of fundamental problems like quantum electrodynamics of strong fields [5-8] and possible direct measurements of vacuum polarization in superheavy systems [5-7]. For the Russian work in the field cf. Ya. B. Zeldovich and Popov [9]. Besides positron autoionization in overcritical fields (decay of the vacuum), one expected particularly also radiative transitions between molecular states if the lifetime of the states is not very much shorter than the elec-

tromagnetic transition time. Estimates show that the collision time is on the order of 10^{-18} sec whereas the $2p - 1s$ transition time is about 10^{-16} sec for a system like Br — Br. Hence roughly 1% of the K-vacancies created in such a collision should give rise to molecular radiation.

In fact, the molecular X-rays have meanwhile been observed by several experimental groups: Saris et al. for the system Ar — Ar [10], Mokler, Stein, and Armbruster for I — Ab [11], MacDonald et al. [12a] for $^{12}C - ^{12}C$, Meyerhof et al. for Br — Br [12b], Burch et al. for Cl — Pb [13], Kaun et al. in the system Ge — Ge [14a], and, most convincingly, Greenberg and Davis for Br — Br and Ni — Ni [15]. The Yale group [15] showed beyond any doubt the very existence of molecular X-rays in heavier ion collisions by investigating and proving the existence of induced radiative transitions, which occur only for radiative molecular transitions (see later).

As mentioned earlier, molecular X-rays are not only an interesting phenomenon in itself but they become a necessary experimental means when the electronic spectra of superheavy elements $(Z > 105)$ are concerned. These elements are of considerable interest in field theory, particularly in Quantum Electrodynamics of Strong Fields. Firstly, the usual perturbative expansion of all QED effects in terms of the coupling constant $Z \alpha$ becomes more than doubtful when Z approaches $\alpha^{-1} \approx 137$. A perturbation expansion in α seems still possible, but not in $Z \alpha$. But proper calculations based on self-consistent field equations as proposed by Reinhard et

al. [16] should be carried out [17] to check the validity of perturbation theory [5, 17]. This theory and its predictions need experimental verification which should be feasible since the QED effects grow much faster with $Z\alpha$ than the electronic transition energies; particularly the vacuum polarization becomes the dominating part of Lamb shift in very strong fields (for estimates see Refs. 5, 17).

Secondly, there is a point where perturbation theory breaks down with certainty, viz. when the lowest bound state (the 1s-state) becomes degenerate with the negative energy continuum states of the Dirac equation [5, 6a]. This happens around $Z \approx 170$, the value with greatest confidence being $Z_{cr} = 172$ [18]. Then the lowest stable ground state of the system, i. e. the vacuum, is no more an unoccupied K-shell, but a doubly occupied K-shell which is imbedded into the negative energy continuum. This new vacuum, the overcritical vacuum is doubly charged [6b, 7]. Whenn an undercritical system with vacant 1s-state is rendered overcritical by increasing the central nuclear charge, the decay of the neutral vacuum shows up by emission of positrons whose energies correspond to the binding energy of the 1s-state minus $2m_ec$ [6a,b]. This should be observable in collisions of, e. g. U — U, where at distances smaller than 35 fm the two nuclei act combined as source of an overcritical electric field. The expected cross sections for positrons have been calculated by Peitz et al. [8] and with inclusion of the non-adiabatic effects in a heavy ion collision by Smith et al. [19]. Cross sections of up to 1/100 barns can be expected.

As no nuclei with a charge $Z > Z_{cr}$ do exist, the experiment has to be done with two colliding heavy ions. For a calculation of the molecular X-ray spectra as well as the expected positron distribution the energy of the molecular states has to be known as a function of the internuclear distance R. This leads us to the wave equation for an electron in the field of two Coulomb centers. For the nonrelativistic equation of the H_2^+-molecule Heitler and London [20] gave the first approximate solution. Exact methods were derived soon after by Teller [21], Hylleraas [22] and Jaffe [23], by expanding the wave functions in terms of a suitable set of basis functions. The equivalence of their methods was shown by Helfrich and Hartmann [24] who also published extensive calculations on the non-relativistic one-electron problem [25]. Many electrons were also taken into account using

Hartree-Fock procedures. We quote only Larkin's calculations of the Ar — Ar system as an example [26].

All these calculations are inappropriate for a system of very heavy ions, the total charge of which is larger than 100. Relativistic effects have to be taken into account. This may be done for light systems, again $Z < 90$, by including relativistic corrections in perturbation theory (expansion in terms of $Z\alpha$) [27]. As $Z\alpha$ approaches 1 this method becomes invalid [69] and breaks down completely for $Z\alpha \geq 1$. In particular the nonrelativistic calculations do not yield negative energy states, which are of fundamental importance for $Z \gtrsim Z_{cr}$.

In addition to the relativistic two center problem, the dynamic aspect of the binary encounter problem in a heavy ion collision is of great importance. Because of the large masses involved, the heavy ion paths can be described classically. The intrinsic (molecular) coordinate system is thus changing as a function of time and hence additional interactions, such as the Coriolis force, will act on the molecular electrons. A semiclassical effect of this will be given in the next Section (II) while Section III deals with the proper covariant transformation of the Dirac equation to rotating frames. No anomaly of the spin with respect to its interaction with the Coriolis field is observed, which would be analogous to the interaction of the spin with a magnetic field (anomalous g-factor).

Sections IV — VII treat, respectively, the technical problems of transforming the two-center-Dirac-equation to elliptical coordinates, elaborating and discussing the constants of motion and — connected with that — the separation of the wavefunctions and the choice of the basis set for the diagonalization procedure. For point charge centers all matrix elements are calculated analytically. All bound state solutions of the two center Dirac equation for single electrons are obtained by diagonalization. The treatment of the finite nuclear dimensions and the numerical procedures are discussed in the next two Sections, VIII and IX. The general features of the level diagrams for both symmetric and asymmetric systems are presented (Section X) and the level-crossing phenomena are discussed (Section XII). In the next two Sections XIII and XIV, we apply the results to determine the "diving point" of the 1s-level (break down point of the neutral vacuum) and present the fully relativistic two center level diagrams.

II. Classical Approximation of the Nuclear Motion

In any heavy ion collision below the Coulomb barrier the relative velocity of target atom and projectile ion is smaller than $c/10$. Therefore, the relative motion of the nuclei of these ions can be treated non-relativistically with a less than 1% error. Then the total Hamiltonian of the system is given by

$$H = (\sum_{i_n} T_{i_n} + \tfrac{1}{2} \sum_{i_n \mp j_n} V_{i_n j_n}) + (\sum_{i_e} D_{i_e} + \tfrac{1}{2} \sum_{i_e \mp j_e} V_{i_e j_e}) + \sum_{i_n j_e} V_{i_n j_e} . \quad (2.1)$$

Here the term enclosed in the first parentheses denotes the kinetic and potential energy operators for the subsystem of the nucleons, the second term in parentheses denotes the relativistic kinetic and potential energy operators for the electron subsystem and the last term describes the interaction between nucleons and electrons. An extensive discussion of a completely quantum mechanical treatment of this Hamiltonian can be found in the article of Smith et alias [28]. As, however, the solution of the full problem does neither seem to be practically feasible at the moment nor worthwhile, we restrict ourselves to cases in which the nuclear part of (2.1) can be dealt with classically.

This is the case if the nucleons can be distributed into two clusters, the two nuclei, and no particle exchange is possible between the clusters. Moreover, we require that the internal wavefunctions of the two nuclei remain unchanged during the whole process. Then, whenever the Sommerfeld parameter [29]

$$\eta = Z_1 Z_2 e^2 / \hbar v \gg 1 , \quad (2.2)$$

a classical treatment of the nuclear motion is possible. For all ion-atom collisions below the Coulomb barrier and Z_1, $Z_2 \gtrsim 5$ this condition is fulfilled; for an $U - U$ collision at the Coulomb barrier one has, e. g. $\eta > 500$. Only in scattering of very light projectiles (e. g. H^+, α-particles) the approximation is not always allowed, but even then the classical trajectories may be used, if the distance of closest approach is larger than about 100 fm.

The assumption of two non-overlapping rigid nuclear clusters leaves us with the simplified Hamiltonian

$$H = \left[\frac{\hat{p}_R^2}{2 M_{red}} + \frac{\hat{L}^2}{2 M_{red} R^2} + V_N(R) \right] + H_e(\boldsymbol{R}) , \quad (2.3)$$

where the term in brackets describes the two naked nuclei (without regard of the influence of the electrons), and $H_e(\boldsymbol{R})$ governs the motion of the electronic cloud and, of course, depends on the relative position of the two nuclei.

The Hamiltonian (2.3) is already denoted in the center-of-mass system. The classical approximation is introduced as follows. The nuclear part of the Hamiltonian (in brackets) is replaced by its classical analog

$$H_{nucl}^{class} = \frac{p_R^2}{2 M_{red}} + \frac{L^2}{2 M_{red} R^2} + V_N(R) , \quad (2.4)$$

where the classical quantities p_R and $\boldsymbol{L}$ are substituted for the operators $\hat{p}_R$ and $\hat{\boldsymbol{L}}$ of relative nuclear motion. The classical Hamiltonian (2.4) can be solved for a Coulomb trajectory $\boldsymbol{R}(t)$ which then is used to eliminate the dynamical variable $\boldsymbol{R}$ from the electronic Hamiltonian H_e.

Unfortunately, $\hat{\boldsymbol{L}}$ is not a conserved quantity since angular momentum may be transferred from the nuclei to the electrons or vice versa. Only the total angular momentem

$$\hat{\boldsymbol{I}} = \hat{\boldsymbol{L}} + \hat{\boldsymbol{J}}_e \quad (2.5)$$

is conserved during the scattering process. Hence we are forced to modify the decoupling scheme of the nuclear variables. We express $\hat{\boldsymbol{L}}$ by $\hat{\boldsymbol{L}} = \hat{\boldsymbol{I}} - \hat{\boldsymbol{J}}_e$ in expression (2.3) and take $\hat{\boldsymbol{I}}$ as a classical quantity $\boldsymbol{I}$. Then we obtain the classical Hamiltonian function for the relative motion of the ions

$$H'^{class}_{nucl} = \frac{p_R^2}{2 M_{red}} + \frac{I^2}{2 M_{red} R^2} + V_N(R) \quad (2.6)$$

and the electronic Hamiltonian plus rotational coupling terms:

$$H = H_e[\boldsymbol{R}(t)] - \frac{\hat{\boldsymbol{I}} \cdot \hat{\boldsymbol{J}}_e}{M_{red} R(t)^2} + \frac{\hat{\boldsymbol{J}}_e^2}{2 M_{red} R(t)^2} . \quad (2.7)$$

The second term indicates the Coriolis coupling between the electrons and the total angular momentum. The third term in (2.7) is a centrifugal potential which is small compared to the Coriolis coupling as mostly $\langle j_e \rangle \ll I$. The derivation of the rotational coupling terms given in this chapter is not rigorous because we have made use only of the non-relativistic kinetic energy operator of the nuclear motion. A rigorous treatment demands to write down the relativistic Hamiltonian for the electrons in a ro-

tating coordinate system, whose z-axis is given by the connecting line of the two nuclei.

III. The Dirac Equation in a Rotating Coordinate System

In order to derive the coupling between rotation and electronic motion from the standpoint of covariance of physical laws, we have to make use of the formulation of the Dirac equation in arbitrary coordinate systems. The generalization of Riemannian space to include spinor variables was developed by Tetrode [30] and by Fock and Ivanenkov [31]. In the notation of Schmutzer [32], the general covariant form of the Dirac equation is

$$\gamma^k \left(\frac{\partial}{\partial x^k} + \Gamma_k - \frac{ie}{\hbar c} A_k \right) \psi + \frac{m_e c}{\hbar} \psi = 0 . \tag{3.1}$$

The γ^k are the Dirac matrices obtained by the commutation relations

$$\gamma^i \gamma^k + \gamma^k \gamma^i = 2 g^{ik} \tag{3.2}$$

and the Γ_k are the spinor connections (i. e. the generalized Christoffel symbols) determined by

$$\Gamma_k = \tfrac{1}{4} \gamma^i (\gamma_{i|k} - \{{}^l_{iK}\} \gamma_l) - \tfrac{1}{32} \text{ trace } (\gamma \gamma^i \gamma_{i|k}) \gamma . \tag{3.3}$$

Here again use has been made of the abbreviation

$$\gamma = \tfrac{1}{24} \varepsilon_{iklm} \gamma^i \gamma^k \gamma^l \gamma^m , \tag{3.4}$$

where ε_{iklm} denotes the totally antisymmetric Levi-Cività tensor. The terms $\partial_k \psi + \Gamma_k \psi$ can be considered as the *covariant derivative of the spinor* ψ.

The metric tensor in a rotating coordinate system is given by

$$g_{ik} = \begin{pmatrix} 1 & 0 & 0 & -\frac{\omega}{c} y \\ 0 & 1 & 0 & \frac{\omega}{c} x \\ 0 & 0 & 1 & 0 \\ -\frac{\omega}{c} y & \frac{\omega}{c} x & 0 & -1 + \frac{\omega^2}{c^2} (x^2 + y^2) \end{pmatrix} \tag{3.5 a}$$

and its inverse by

$$g^{ik} = \begin{pmatrix} 1 - \left(\frac{\omega}{c} y\right)^2 & \frac{\omega^2}{c^2} x y & 0 & -\frac{\omega}{c} y \\ \frac{\omega^2}{c^2} x y & 1 - \left(\frac{\omega}{c} x\right)^2 & 0 & \frac{\omega}{c} x \\ 0 & 0 & 1 & 0 \\ -\frac{\omega}{c} y & \frac{\omega}{c} x & 0 & -1 \end{pmatrix} \tag{3.5 b}$$

Here the z-axis is chosen to be the axis of rotation. Denoting by $\hat\gamma_i$ the Dirac matrices associated with this rotating intrinsic frame of reference and by γ_i those of the ordinary Lorentz metric, one finds from (3.2)

$$\hat\gamma_i = \left\{ \gamma_1, \gamma_2, \gamma_3, \gamma_4 + \frac{\omega}{c} x \gamma_2 - \frac{\omega}{c} y \gamma_1 \right\} = \left\{ \boldsymbol{\gamma}, \gamma_4 + \left(\frac{\boldsymbol{\omega}}{c} \times \boldsymbol{r}\right) \cdot \boldsymbol{\gamma} \right\}, \tag{3.6 a}$$

$$\hat\gamma^i = \left\{ \gamma_1 - \frac{\omega}{c} y \gamma_4, \gamma_2 + \frac{\omega}{c} x \gamma_4, \gamma_3, -\gamma_4 \right\} = \left\{ \boldsymbol{\gamma} + \left(\frac{\boldsymbol{\omega}}{c} \times \boldsymbol{r}\right) \gamma_4, -\gamma_4 \right\} \tag{3.6 b}$$

where also the three dimensional vector notation has been used.

With these preliminaries one can straightforwardly evaluate the connections (3.3) and finds

$$\hat\gamma_k \Gamma_k = \frac{1}{4} \gamma_4 \frac{\boldsymbol{\omega}}{c} \cdot (\boldsymbol{\gamma} \times \boldsymbol{\gamma}) - \frac{1}{4} \left(\frac{\dot{\boldsymbol{\omega}}}{c^2} \times \boldsymbol{r}\right) \cdot \boldsymbol{\gamma} \tag{3.7}$$

where, again, vector notation was applied to express the result. For all details of the calculation we refer to Appendix A.

We substitute this result into the Dirac Eq. (3.1) and find

$$(\boldsymbol{\gamma} \cdot \nabla) \psi + \gamma_4 \left(\frac{\boldsymbol{\omega}}{c} \times \boldsymbol{r}\right) \cdot \nabla \psi - \frac{1}{c} \gamma_4 \frac{\partial \psi}{\partial t} + \gamma_4 \frac{ie}{\hbar c} A_4 \psi - \frac{ie}{\hbar c} \left[\boldsymbol{\gamma} + \left(\frac{\boldsymbol{\omega}}{c} \times \boldsymbol{r}\right) \gamma_4 \right] \cdot \boldsymbol{A}$$
$$+ \frac{1}{4} \gamma_4 \frac{\boldsymbol{\omega}}{c} \cdot (\boldsymbol{\gamma} \times \boldsymbol{\gamma}) \psi - \frac{1}{4} \left(\frac{\dot{\boldsymbol{\omega}}}{c^2} \times \boldsymbol{r}\right) \cdot \boldsymbol{\gamma} \psi + \frac{m_e c}{\hbar} \psi = 0 . \tag{3.8}$$

Multiplication of Eq. (3.8) by $-i \hbar c \gamma_4$ and use of the definitions $\gamma_4 \boldsymbol{\gamma} = \boldsymbol{\alpha}$ and $-i \gamma_4 = \beta$ gives

$$i \hbar \frac{\partial \psi}{\partial t} = \left[c \boldsymbol{\alpha} \cdot \left(\boldsymbol{p} - \frac{e}{c} \boldsymbol{A} \right) + V + \beta m_e c^2 \right] \psi - (\boldsymbol{\omega} \times \boldsymbol{r}) \cdot \left(\boldsymbol{p} - \frac{e}{c} \boldsymbol{A} \right) \psi - \tfrac{1}{2} \hbar \boldsymbol{\omega} \cdot \boldsymbol{\sigma} \psi + \frac{i \hbar}{4} \left(\frac{\dot{\boldsymbol{\omega}}}{c^2} \times \boldsymbol{r} \right) \cdot \boldsymbol{\alpha} \psi . \tag{3.9}$$

In our notation we have $V = -e A_4$.

The first term in Eq. (3.9) is just the Dirac equation in an inertial frame of reference. All additional terms vanish to $|\boldsymbol{\omega}| = 0$ and have thus to be attributed to the rotation. Again, the terms

$$- (\boldsymbol{\omega} \times \boldsymbol{r}) \cdot (\boldsymbol{p} - (e/c) \boldsymbol{A}) \psi - \hbar \, \boldsymbol{\omega} \cdot \boldsymbol{\sigma} \, \psi = - \boldsymbol{\omega} \cdot [(\boldsymbol{r} \times \boldsymbol{p}) + \tfrac{1}{2} \hbar \, \boldsymbol{\sigma}] \psi + (e/c) (\boldsymbol{\omega} \times \boldsymbol{r}) \cdot \boldsymbol{A} \, \psi \qquad (3.10)$$

can be interpreted as the Coriolis coupling of electronic and rotational motion. The first term is the same as the interaction in (2.7). It is interesting to note that the spin couples in the same way to the rotation as the orbital angular momentum does. If, instead of a rotation we would introduce a magnetic field B the equation would read:

$$i \hbar \, \partial \psi / \partial t = [c \, \boldsymbol{\alpha} \cdot (\boldsymbol{p} - (e/2 \, c) (\boldsymbol{B} \times \boldsymbol{r})) + \beta \, m_{\mathrm{e}} \, c^2] \psi \qquad (3.11)$$

which in the nonrelativistic limit reduces to

$$i \hbar \frac{\partial \psi}{\partial t} \sim \left[\frac{\boldsymbol{p}^2}{2 \, m_{\mathrm{e}}} - \frac{e}{2 \, m_{\mathrm{e}} \, c} (\boldsymbol{B} \times \boldsymbol{r}) - \frac{e \, \hbar}{2 \, m_{\mathrm{e}} \, c} \boldsymbol{\sigma} \cdot \boldsymbol{B} \right] \psi \qquad (3.12)$$

whereas the free Dirac equation with rotation reduces to

$$i \hbar \, \partial \psi / \partial t \sim [\boldsymbol{p}^2 / 2 \, m_{\mathrm{e}} - (\boldsymbol{\omega} \times \boldsymbol{r}) - (\hbar / 2) \, \boldsymbol{\sigma} \cdot \boldsymbol{\omega}] \psi . \qquad (3.13)$$

The identification $\omega = (e/2 \, m_{\mathrm{e}} c) B$ equates Coriolis and Lorentz force in (3.12) and (3.13), but the coupling to the electron spin differs by a factor two. This seems to destroy the analogy between a field of rotation and a uniform magnetic field for particles with spin. However, it is easy to see that the Coriolis coupling must be $(- \boldsymbol{\omega} \cdot \boldsymbol{j})$ to the total angular momentum $\boldsymbol{j}$. If ψ is a solution in the inertial reference frame, then it should be

$$\psi' = \exp \{ (i/\hbar) \, \boldsymbol{\Theta} \cdot \boldsymbol{j} \} \, \psi \qquad (3.14)$$

in the rotated (rotating) frame. This is actually true since:

$$i \hbar \frac{\partial}{\partial t} \psi' = \exp \{ (i/\hbar) \, \boldsymbol{j} \cdot \boldsymbol{\Theta} \} \left[i \hbar \frac{\partial}{\partial t} \psi - \dot{\boldsymbol{\Theta}} \cdot \boldsymbol{j} \, \psi \right]$$

$$= \exp \{ (i/\hbar) \, \boldsymbol{j} \cdot \boldsymbol{\Theta} \} [H_{\mathrm{Lab}} - \boldsymbol{\omega} \cdot \boldsymbol{j}] \, \psi$$

$$= [H_{\mathrm{Lab}} - \boldsymbol{\omega} \cdot \boldsymbol{j}] \, \psi' \qquad (3.15)$$

provided the Hamiltonian commutes with $\boldsymbol{\Theta} \cdot \boldsymbol{j}$. Thus the rotated wave function is a solution to the wave equation in the rotating frame. This is not a trivial result, since (3.14) was only derived for time independent rotations (Lorentz-transformations) and not for rotations with constant angular velocity.

We also want to point out, that the expectation values for stationary states

$$\langle \psi \, | \, i \hbar \, \partial / \partial t \, | \, \psi \rangle = E , \qquad \langle \psi \, | - i \hbar \nabla \, | \, \psi \rangle = \boldsymbol{p} \qquad (3.16)$$

form a covariant four-vector. The contravariant energy-momentum vector $(\boldsymbol{\pi}, E')$ instead is seen to be

$$E' = E + (\boldsymbol{\omega} \times \boldsymbol{r}) \cdot \boldsymbol{p} , \qquad \boldsymbol{\pi} = \boldsymbol{p} - (\boldsymbol{\omega}/c^2) \times \boldsymbol{r} . \qquad (3.17)$$

These quantities transform between the rotating and the laboratory system as expected:

$$E'_{\mathrm{Lab}} = E'_{\mathrm{rot}} , \qquad \boldsymbol{\pi}_{\mathrm{Lab}} = \boldsymbol{\pi}_{\mathrm{rot}} + m_{\mathrm{e}} (\boldsymbol{\omega} \times \boldsymbol{r}) . \qquad (3.18)$$

The coupling to the electromagnetic field

$$H_{\mathrm{rad}} = - e A_4 - e \, \boldsymbol{\alpha} \cdot \boldsymbol{A} + (e/c) (\boldsymbol{\omega} \times \boldsymbol{r}) \cdot \boldsymbol{A} \qquad (3.19)$$

can be understood from the general minimal coupling prescription $\gamma^\varkappa A_\varkappa$ and the special form of the $\gamma^\varkappa$ matrices (3.6 b). The last terms in Eq. (3.19) was interpreted by the authors as an additional "induced" coupling to the radiation field [33, 34]. However, one has to bear in mind that the $A_\varkappa$-field in (3.19) is the one seen in the rotating system. If the radiation field is quantized in the transverse gauge in the lab system

$$A^\varkappa_{\mathrm{lab}} = \{ \boldsymbol{\varepsilon} \, e^{i \boldsymbol{k} \cdot \boldsymbol{x}}, 0 \} , \qquad \boldsymbol{\varepsilon} \cdot \boldsymbol{k} = 0 \qquad (3.20)$$

then in the rotating system

$$A_\varkappa = \{ \boldsymbol{\varepsilon} \, e^{i \boldsymbol{k} \cdot \boldsymbol{x}}, \quad \boldsymbol{\varepsilon} \cdot (\boldsymbol{\omega}/c \times \boldsymbol{r}) \, e^{i \boldsymbol{k} \cdot \boldsymbol{x}} \} , \qquad (3.21)$$

and the resulting coupling is simply

$$H_{\mathrm{rad}} = - e \, \boldsymbol{\alpha} \cdot \boldsymbol{\varepsilon} \, e^{i \boldsymbol{k} \cdot \boldsymbol{x}} , \qquad (3.22)$$

and no additional contribution from the rotation is left.

IV. Constants of Motion

In order to find analytic or semi-analytic solutions of a wave equation and to reduce the degrees of freedom, it is important to know the constants of motion, i. e. the operators that commute with the Hamiltonian. From now on we deal with the Hamiltonian

$$H = c \, \boldsymbol{\alpha} \cdot \boldsymbol{p} + \beta \, m_{\mathrm{e}} \, c^2 + V_1(r_1) + V_2(r_2) \qquad (4.1)$$

where the two central potentials V_1 and V_2 may be different. Obviously, (4.1) has cylindrical symmetry and therefore one would expect the projection of the angular momentum $\boldsymbol{J} = (\boldsymbol{L} + (\hbar/2)\,\boldsymbol{\sigma})$ on the z-axis to be a constant of motion. One easily finds:

$$[H, \beta J_z]_- = [V_1(r_1) + V_2(r_2), \beta J_z]_- \qquad (4.2)$$
$$= [V_1(r), \beta J_z]_- + [V_2(r_2), \beta J_z]_- = 0,$$

because βJ_z commutes with each of the two central potentials. The essential assumption is that both V_1 and V_2 have their centers on the z-axis which is the projection axis of J_z. This is not fulfilled for J_x and J_y. Hence the total angular momentum operator J^2 does not commute with H.

However, for the corresponding nonrelativistic Hamiltonian,

$$H_{\mathrm{nonrel}} = p^2/2\,m_e + V_1(r_1) + V_2(r_2) \qquad (4.3)$$

it is possible to construct an operator which can replace the total angular momentum operator for certain potentials V_1 and V_2. The general form of the potential which permits this construction is [35, 36]

$$\left. \begin{array}{l} V_1(r_1) = \tfrac{1}{2} k\, r_1{}^2 - Z_1\, e^2/r_1 + \mathrm{const} \\ V_2(r_2) = \tfrac{1}{2} k\, r_2{}^2 - Z_2\, e^2/r_2 + \mathrm{const} \end{array} \right\}. \qquad (4.4)$$

The oscillator part is trivial, since for equal k the two oscillators add up to a single oscillator with strength $k\sqrt{2}$ and located at the center between the two original potential origins. For the part with physical relevance

$$V_1(r_1) + V_2(r_2) = -Z_1\, e^2/r_1 - Z_2\, e^2/r_2 \qquad (4.5)$$

the constant of motion was first given by Erikson and Hill [35] (see Fig. 1)

$$A = \tfrac{1}{2}(\boldsymbol{L}_1 \cdot \boldsymbol{L}_2 + \boldsymbol{L}_2 \cdot \boldsymbol{L}_1) \qquad (4.6)$$
$$- 2\, m_e\, R\,(Z_1\, e^2 \cos \Theta_1 - Z_2\, e^2 \cos \Theta_2),$$

where $2R$ is the distance between the centers, Θ_1 and Θ_2 the angles between r_1 and the z-axis resp. r_2 and the z-axis. $\boldsymbol{L}_1$ and $\boldsymbol{L}_2$ are the angular momentum operators with respect to the two centers. It was stated by Coulson and Joseph [35] that an analogous operator cannot be constructed for the relativistic case, but to our knowledge this has not been proven before. It is difficult to show that the construction is impossible. However, one can show that all straightforward generalizations of (4.6) fail to commute with the Hamiltonian (4.1): Certainly, the orbital angular momentum $\boldsymbol{L}$ has to be replaced

by the total angular momentum $\boldsymbol{j}$. Then we consider

$$A = \tfrac{1}{2}[\boldsymbol{J}_1 \cdot \boldsymbol{J}_2 + \boldsymbol{J}^2 \cdot \boldsymbol{J}_1] \qquad (4.7)$$
$$= \tfrac{1}{2}[\boldsymbol{L}_1 \cdot \boldsymbol{L}_2 + \boldsymbol{L}_2 \cdot \boldsymbol{L}_1] + \tfrac{1}{2}\hbar\,\boldsymbol{\sigma} \cdot [\boldsymbol{L}_1 + \boldsymbol{L}_2] + \tfrac{3}{4}\hbar^2.$$

One easily sees that A commutes with

$$D = c\,\boldsymbol{\alpha} \cdot \boldsymbol{p} + \beta\, m_e\, c^2 \qquad (4.8)$$

since this holds for $\beta\boldsymbol{J}$, and $\beta\boldsymbol{J}_2$ each. An elementary calculation gives

$$[A, V_1(r_1)] = 2\,\hbar^2\, R\, V_1{}'(r_1)\cos\Theta_1$$
$$+ i\,\hbar^2\, R\,\boldsymbol{\sigma} \cdot (\boldsymbol{e}_z \times \nabla) V_1(r_1)$$
$$= i\,\hbar\, R\,(a_z\,\boldsymbol{\alpha} \cdot \boldsymbol{p} + p_z) V_1(r_1). \qquad (4.9)$$

Now one would have to find an operator $F_1(r_1)$ which commutes with $V_1(r_1)$ and

$$[D, F_1(r_1)] = [A, V_1(r_1)]. \qquad (4.10)$$

A simple function $f_1(r_1) = F_1(r_1)$ is not a suitable choice since then

$$[D, f_1(r_1)] = c\,\boldsymbol{\alpha} \cdot \boldsymbol{p}\, f_1(r). \qquad (4.11)$$

In order to account for the a_z factor in (4.9) one would like to choose

$$F_1(r_1) = a_z\, f_1(r_1)$$

but then additional commutators like $[\boldsymbol{\alpha}, a_z]_-\, f_1(r_1) \cdot \boldsymbol{p}$ occur. If one tried to eliminate the disturbing a_z already in Eq. (4.9) one has tot take $a_z A$ instead of A, but then one faces $[a_z A, D]_- \neq 0$. Thus every possible construction of a constant of motion in the relativistic problem fails.

For a special class of two center problems, there is, however, an additional symmetry. Whenever the two central potentials are alike, i. e. whenever we deal with identical nuclei, the relativistic parity operator, βP, commutes with H (4.1). That βP commutes with D (4.8) is well known [37]. Furthermore, we have

$$P(\boldsymbol{r}_1) = -\boldsymbol{r}_2 \quad \text{and} \quad P(\boldsymbol{r}_2) = -\boldsymbol{r}_1 \qquad (4.12)$$

if the center of the inversion is taken to be the median point of the line connecting the two potential centers (which in the case of symmetry happens to be the center-of-mass). For $V_1 = V_2$ it follows that

$$[V_1(r_1) + V_2(r_2), \beta P]_- = \beta[V_1(r_1) - V_2(r_1) \qquad (4.13)$$
$$+ V_2(r_2) - V_1(r_2)] \equiv 0.$$

Accordingly, the relativistic molecular orbitals can be classified with respect of the quantum number m

of j_z:

$$j_z \, \psi_m(\boldsymbol{r}) = m \, \psi(\boldsymbol{r}) \qquad (4.14)$$

and in the case of symmetric system also with respect to parity, i.e. we have either "gerade" states of even or "ungerade" states of odd parity. The value of m is commonly denoted by Greek letters σ, π, δ, ... for $m = \pm\frac{1}{2}$, $\pm\frac{3}{2}$, $\pm\frac{5}{2}$, ...; the parity by an index g or u. States of same cylindrical symmetry and parity are identified by the quantum numbers of the asymptotic atomic state they tend to when the nuclear separation vanishes, e.g. $1s_{1/2}\,\sigma_g$, $3p_{3/2}\tau_u$, etc.

V. Transformation to Spheroidal Coordinates

The appropriate coordinate system for a two center problem is defined by prolate spheroidal coordinates ξ, η, φ, which are connected with Cartesian coordinates via the equations

$$\left. \begin{aligned} x &= R\,\sqrt{(\xi^2-1)(1-\eta^2)}\,\cos\varphi, \\ y &= R\,\sqrt{(\xi^2-1)(1-\eta^2)}\,\sin\varphi, \\ z &= R\,\xi\,\eta, \end{aligned} \right\} \qquad (5.1)$$

and especially ξ and η are defined as (Fig. 1)

$$\xi = (r_1 + r_2)/2\,R, \qquad \eta = (r_1 - r_2)/2\,R. \qquad (5.2)$$
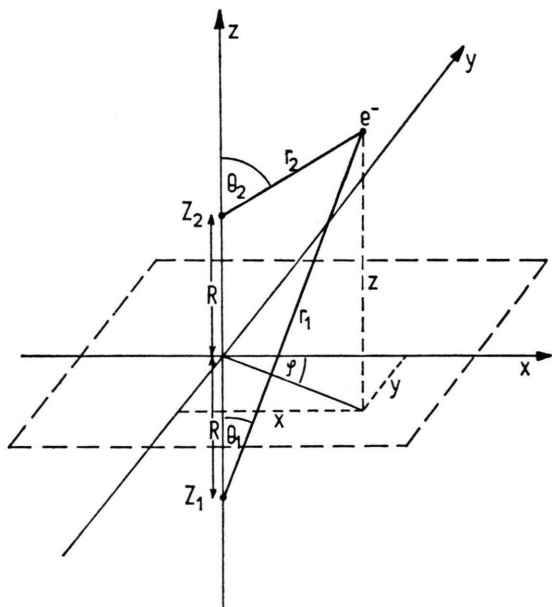
Fig. 1. The connection between Cartesian and elliptical (spheroidal) coordinates.

The coordinates are defined in the region

$$1 \leqq \xi < \infty, \qquad -1 \leqq \eta \leqq +1, \qquad 0 \leqq \varphi < 2\pi. \qquad (5.3)$$

According to the general rule the quantization has to be carried out in Cartesian coordinates and only afterwards transformation into curvilinear coordinates is permitted. We start from the Dirac equation without coupling terms

$$(c\,\boldsymbol{\alpha}\cdot\boldsymbol{p} + \beta\,m_e\,c^2 - Z_1\,e^2/r_1 - Z_2\,e^2/r_2 - E)\,\psi(\boldsymbol{r}) = 0, \qquad (5.4)$$

and use the following representation of Dirac's matrices [38]

$$\boldsymbol{\alpha} = \begin{pmatrix} 0 & \boldsymbol{\sigma} \\ \boldsymbol{\sigma} & 0 \end{pmatrix}, \qquad \beta = \begin{pmatrix} I & 0 \\ 0 & -I \end{pmatrix}, \qquad (5.5)$$

for the Pauli matrices

$$\boldsymbol{\sigma} = \left\{ \begin{pmatrix} 0 & 1 \\ 1 & 0 \end{pmatrix}, \begin{pmatrix} 0 & -i \\ i & 0 \end{pmatrix}, \begin{pmatrix} 1 & 0 \\ 0 & -1 \end{pmatrix} \right\} \qquad (5.6)$$

and for the momentum operator

$$\boldsymbol{p} = -i\,\hbar\,\nabla = -i\,\hbar \left\{ \frac{\partial}{\partial x}, \quad \frac{\partial}{\partial y}, \quad \frac{\partial}{\partial z} \right\}. \qquad (5.7)$$

In the prolate spheroidal coordinate system with the orthogonal unit vectors $\boldsymbol{u}_\xi$, $\boldsymbol{u}_\eta$, $\boldsymbol{u}_\varphi$ the gradient operator reads [39]

$$\nabla = \frac{\boldsymbol{u}_\xi}{e_\xi}\,\frac{\partial}{\partial\xi} + \frac{\boldsymbol{u}_\eta}{e_\eta}\,\frac{\partial}{\partial\eta} + \frac{\boldsymbol{u}_\varphi}{e_\varphi}\,\frac{\partial}{\partial\varphi} \qquad (5.8)$$

where the normalization factors are given by

$$\left. \begin{aligned} e_\xi &= \left| \frac{\partial\boldsymbol{r}}{\partial\xi} \right| = R\left(\frac{\xi^2-\eta^2}{\xi^2-1} \right)^{1/2}, \\ e_\eta &= \left| \frac{\partial\boldsymbol{r}}{\partial\eta} \right| = R\left(\frac{\xi^2-\eta^2}{1-\eta^2} \right)^{1/2}, \\ e_\varphi &= \left| \frac{\partial\boldsymbol{r}}{\partial\varphi} \right| = R\,\sqrt{(\xi^2-1)(1-\eta^2)}. \end{aligned} \right\} \qquad (5.9)$$

A vector $\boldsymbol{a}$ obtains the form

$$\boldsymbol{a} = a_\xi\,\boldsymbol{u}_\xi + a_\eta\,\boldsymbol{u}_\eta + a_\varphi\,\boldsymbol{u}_\varphi \qquad (5.10)$$

with the new components

$$a_\xi = \frac{1}{e_\xi}\left(\boldsymbol{a}\cdot\frac{\partial\boldsymbol{r}}{\partial\xi} \right), \quad \text{etc.} \qquad (5.11)$$

After these preliminaries one easily calculates the Dirac operator of kinetic energy in spheroidal co-

ordinates to be

$$\boldsymbol{\alpha}\cdot\nabla = \frac{a_\xi}{e_\xi}\frac{\partial}{\partial\xi} + \frac{a_\eta}{e_\eta}\frac{\partial}{\partial\eta} + \frac{a_\varphi}{e_\varphi}\frac{\partial}{\partial\varphi} = \frac{(a_x\cos\varphi + a_y\sin\varphi)\,\xi\,W(\xi,\eta) + a_z\,\eta\,(\xi^2-1)}{R(\xi^2-\eta^2)}\frac{\partial}{\partial\xi}$$

$$+ \frac{-(a_x\cos\varphi + a_y\sin\varphi)\,\eta\,W(\xi,\eta) + a_z\,\xi\,(1-\eta^2)}{R(\xi^2-\eta^2)}\frac{\partial}{\partial\eta} + \frac{-a_x\sin\varphi + a_y\cos\varphi}{R\,W(\xi,\eta)}\frac{\partial}{\partial\varphi}\,. \quad (5.12)$$

Using the representation of the α-matrices (5.5) given above, we find

$$\boldsymbol{\alpha}\cdot\boldsymbol{p} = \begin{pmatrix} 0 & 0 & p_z & p_x - i\,p_y \\ 0 & 0 & p_x + i\,p_y & -p_z \\ p_z & p_x - i\,p_y & 0 & 0 \\ p_x + i\,p_y & -p_z & 0 & 0 \end{pmatrix} \quad (5.13)$$

with the momentum operator components

$$p_x \pm i\,p_y = \frac{-i\,\hbar\,e^{\pm i\varphi}}{R(\xi^2-\eta^2)}\left[W(\xi,\eta)\left(\xi\frac{\partial}{\partial\xi} - \eta\frac{\partial}{\partial\eta}\right)\right.$$
$$\left. \pm \frac{i}{W(\xi,\eta)}(\xi^2-\eta^2)\frac{\partial}{\partial\varphi}\right],$$
$$p_z = \frac{-i\,\hbar}{R(\xi^2-\eta^2)}\left[\eta(\xi^2-1)\frac{\partial}{\partial\xi}\right.$$
$$\left. + \xi(1-\eta^2)\frac{\partial}{\partial\eta}\right]. \quad (5.14)$$

In Eqs. (5.12) and (5.14) the abbreviation

$$W(\xi,\eta) = e_\varphi/R = [(\xi^2-1)(1-\eta^2)]^{1/2} \quad (5.15)$$

was introduced.

Finally, we have to transcribe the potentials. For the special case of two point charges $Z_1\,e$ resp. $Z_2\,e$, which we choose to be the foci of the spheroidal coordinate system we obtain

$$V(\boldsymbol{r}) = \frac{-Z_1\,e^2}{r_1} - \frac{Z_2\,e^2}{r_2}$$
$$= -\frac{e^2}{R}\frac{(Z_1+Z_2)\,\xi + (Z_2-Z_1)\,\eta}{(\xi^2-\eta^2)}\,. \quad (5.16)$$

The common feature of all operators (5.14) and (5.16) is that they have a denominator $R(\xi^2-\eta^2)$. In prolate spheroidal coordinates the volume element is given by [39]

$$d^3x = R^3(\xi^2-\eta^2)\,d\xi\,d\eta\,d\varphi\,. \quad (5.17)$$

Therefore, in all matrix elements with any of the above operators the denominator is cancelled and only polynomials remain. This will allow analytical integration of these matrix elements in Section VII.

VI. Reduction to a Two Dimensional Problem

We have shown in Sect. IV that the cylindrical symmetry of the two center problem implies that the angular momentum projection J_z is a good quantum number of the molecular states. Therefore, it is possible to represent the wavefunctions in the φ-variable by a suitable combination of exponentials. Besides, the wave Eq. (5.1) has singularities at all points with $\xi = 1$, i.e. at the two foci and all intermediate points. If we include the singular behavior, the appropriate form of the wavefunctions for a particular $m = \langle J_z \rangle$ is

$$\Psi_m(\xi,\eta,\varphi)$$
$$= \begin{pmatrix} (\xi^2-1)^{\frac{1}{2}|m-\frac{1}{2}|}\exp\{i(m-\frac{1}{2})\varphi\}\;\psi_1(\xi,\eta) \\ (\xi^2-1)^{\frac{1}{2}|m+\frac{1}{2}|}\exp\{i(m+\frac{1}{2})\varphi\}\;\psi_2(\xi,\eta) \\ i(\xi^2-1)^{\frac{1}{2}|m-\frac{1}{2}|}\exp\{i(m-\frac{1}{2})\varphi\}\;\psi_3(\xi,\eta) \\ i(\xi^2-1)^{\frac{1}{2}|m+\frac{1}{2}|}\exp\{i(m+\frac{1}{2})\}\;\psi_4(\xi,\eta) \end{pmatrix} \quad (6.1)$$

The Ansatz (6.1) is in analogy to the wavefunctions used in the nonrelativistic problem [22, 23] and allowance was made for the different coupling between spin and orbital angular momentum in the various spinor components. One easily verifies that (6.1) in fact is an eigenfunction to $J_z = L_z + \frac{1}{2}\hbar\,\sigma_z$:

$$J_z\,\Psi_m(\xi,\eta,\varphi) = \left\{-i\,\hbar\frac{\partial}{\partial\varphi} + \frac{\hbar}{2}\begin{pmatrix}1 & & & \\ & -1 & & \\ & & 1 & \\ & & & -1\end{pmatrix}\right\}\Psi_m(\xi,\eta,\varphi) = m\,\hbar\,\Psi_m(\xi,\eta,\varphi)\,. \quad (6.2)$$

We now proceed to the consequences of (6.1) upon the Dirac equation, whereby we restrict ourselves to the case $m > 0$. It is sufficient to explore the action of $\boldsymbol{\alpha}\cdot\boldsymbol{p}$ on $\Psi_m(\xi,\eta,\varphi)$:

$$(p_x + i\,p_y)\left[(\xi^2-1)^{(\frac{1}{2}m-\frac{1}{4})}\exp\{i(m-\frac{1}{2})\varphi\}\,f(\xi,\eta)\right] = \frac{-i\,\hbar}{R(\xi^2-\eta^2)}(\xi^2-1)^{\frac{1}{2}m+\frac{1}{4}}\exp\{i(m+\frac{1}{2})\varphi\}\cdot \quad (6.3)$$

$$\cdot\left[\sqrt{1-\eta^2}\left(\xi\frac{\partial}{\partial\xi} - \eta\frac{\partial}{\partial\eta}\right) - \frac{(m-\frac{1}{2})\eta^2}{\sqrt{1-\eta^2}}\right]f(\xi,\eta)\,,$$

$$(p_x + i\, p_y)\,[\,(\xi^2 - 1)^{(\frac{1}{2}m - \frac{1}{4})}\exp\{i(m + \tfrac{1}{2})\varphi\}\,f(\xi,\eta)\,] = \frac{-i\,\hbar}{R(\xi^2 - \eta^2)}\exp\{i(m - \tfrac{1}{2})\varphi\}\,(\xi^2 - 1)^{\frac{1}{2}m - \frac{1}{4}} \qquad (6.4)$$

$$\cdot\left[\sqrt{1 - \eta^2}\left((2m + 1)\,\xi^2 + (\xi^2 - 1)\left(\xi\frac{\partial}{\partial\xi} - \eta\frac{\partial}{\partial\eta}\right)\right) + \frac{(m + \frac{1}{2})\eta^2}{\sqrt{1 - \eta^2}}(\xi^2 - 1)\right]f(\xi,\eta)\,,$$

$$p_z\,[\,(\xi^2 - 1)^{\frac{1}{2}m \pm \frac{1}{4}}\exp\{i(m \pm \tfrac{1}{2})\varphi\}f(\xi,\eta)\,] = \frac{-i\,\hbar}{R(\xi^2 - \eta^2)}(\xi^2 - 1)^{\frac{1}{2}m \pm \frac{1}{4}}\exp\{i(m \pm \tfrac{1}{2})\varphi\}\cdot \qquad (6.5)$$

$$\cdot\left[(m \pm \tfrac{1}{2})\,\xi\,\eta + \eta(\xi^2 - 1)\frac{\partial}{\partial\xi} + \xi(1 - \eta^2)\frac{\partial}{\partial\eta}\right]f(\xi,\eta)\,.$$

Inserting these results into the expression (5.13) of the operator $\boldsymbol{\alpha}\cdot\boldsymbol{p}$ and noting $X = (\xi^2 - 1)$ as abbreviation we are left with

$$(\boldsymbol{\alpha}\cdot\boldsymbol{p})\,\Psi_m(\xi,\eta,\varphi) = \Phi_m\,\pi_m\,\psi(\xi,\eta) \qquad (6.6)$$

where the matrix operators Φ_m are [with $\Sigma = \exp(i\,\varphi)\,X$]:

$$\Phi_m = \begin{pmatrix} \Sigma^{m - \frac{1}{2}} & 0 & 0 & 0 \\ 0 & \Sigma^{m + \frac{1}{2}} & 0 & 0 \\ 0 & 0 & i\,\Sigma^{m - \frac{1}{2}} & 0 \\ 0 & 0 & 0 & i\,\Sigma^{m + \frac{1}{2}} \end{pmatrix} \qquad (6.7)$$

and

$$\pi_m = \begin{pmatrix} 0 & 0 & -\pi_{z-} & -\pi_- \\ 0 & 0 & -\pi_+ & \pi_{z+} \\ \pi_{z-} & \pi_- & 0 & 0 \\ \pi_+ & -\pi_{z+} & 0 & 0 \end{pmatrix}. \qquad (6.8)$$

Matrix formulation has been used to commute the differential operators π_+, π_-, π_{z+} and π_{z-} with the φ-dependent part of the wave function. These operators are

$$\left.\begin{aligned}
\pi_+ &= \frac{-\hbar}{R(\xi^2 - \eta^2)}\left[\sqrt{1 - \eta^2}\left(\xi\frac{\partial}{\partial\xi} - \eta\frac{\partial}{\partial\eta}\right) - \frac{(m - \frac{1}{2})\eta^2}{\sqrt{1 - \eta^2}}\right], \\
\pi_- &= \frac{-\hbar}{R(\xi^2 - \eta^2)}\left[\sqrt{1 - \eta^2}\left((2m + 1)\xi^2 + \xi(\xi^2 - 1)\frac{\partial}{\partial\xi} - (\xi^2 - 1)\eta\frac{\partial}{\partial\eta} + \frac{(m + \frac{1}{2})\eta^2}{\sqrt{1 - \eta^2}}\right)\right], \\
\pi_{z\pm} &= \frac{-\hbar}{R(\xi^2 - \eta^2)}\left[(m \pm \tfrac{1}{2})\xi\,\eta + \eta(\xi^2 - 1)\frac{\partial}{\partial\xi} + \xi(1 - \eta^2)\frac{\partial}{\partial\eta}\right].
\end{aligned}\right\} \qquad (6.9)$$

Formulae (6.6) and (6.9) can be checked by elementary but rather cumbersome calculations.

We are now ready to formulate the Dirac Eq. (5.1) in a more convenient way in prolate spheroidal coordinates, where the variable ψ is already split off:

$$(c\,\boldsymbol{\alpha}\cdot\boldsymbol{p} + \beta\,m_e\,c^2 - Z_1\,e^2/r_1 - Z_2\,e^2/r_2 - E)\,\Psi(\boldsymbol{r}) \qquad (6.10)$$

$$= \Phi_m\left(c\,\pi_m + \beta\,m_e\,c^2 - \frac{e^2}{R}\frac{(Z_1 + Z_2)\,\xi - (Z_1 - Z_2)\,\eta}{(\xi^2 - \eta^2)} - E\right)\psi(\xi,\eta) = 0\,.$$

Observe that the total spinor has the structure

$$\Psi(\boldsymbol{r}) = \Psi_m(\xi,\eta,\varphi) = \Phi_m\,\psi(\xi,\eta) \quad (6.11)$$

and that two diagonal matrices (Φ_m,β) always commute.

Up to now the case $m < 0$ has been explicitly excluded. However, the Dirac equation must have the same eigenvalues for $m = \pm|m|$ on grounds of symmetry arguments. A switch from m to $-m$ corresponds to a transformation of J_z to $-J_z$ which can be represented by

$$\varphi \to -\varphi \quad \text{and} \quad \sigma_z \to -\sigma_z = U\,\sigma_z\,U^+ \quad (6.12)$$

with the unitary matrix

$$U = \sigma_x = \begin{pmatrix} 0 & 1 & 0 & 0 \\ 1 & 0 & 0 & 0 \\ 0 & 0 & 0 & 1 \\ 0 & 0 & 1 & 0 \end{pmatrix}. \qquad (6.13)$$

With Eq. (6.1) one immediately checks that

$$\Psi_{-m}(\xi,\eta,\varphi) = U\,\Psi_m(\xi,\eta,-\varphi)\,. \qquad (6.14)$$

Besides, we need the transformation properties of the Hamiltonian under the transformation (6.12). The terms in (5.4) are invariant except $\boldsymbol{\alpha} \cdot \boldsymbol{p}$ (e.g. $U \beta U^+ = \beta$). Next, $\varphi \to -\varphi$ induces the changes

$$p_x + i p_y \longleftrightarrow p_x - i p_y, \quad p_z \to -p_z \quad (6.15)$$

because $(\xi^2 - \eta^2)$ and $W(\xi, \eta)$ change signs (the new system is lefthanded). A short calculation then shows that

$$H(\varphi) = U H(-\varphi) U^+ \quad (6.16)$$

and we have proved that

$$\begin{aligned} H(\varphi) \Psi_{-m}(\xi, \eta, \varphi) &= U H(-\varphi) U^+ U \Psi_m(\xi, \eta, -\varphi) \\ &= U H(-\varphi) \Psi_m(\xi, \eta, -\varphi) . \end{aligned}$$
$$(6.17)$$

This means that $m = \pm |m|$ yields the same eigenvalues and the eigenfunctions for negative m-values are most easily obtained from those for positive ones through the relation (6.14). Therefore, it is sufficient to solve the two-center Dirac equation for positive values m of the angular momentum projection onto the nuclear axis.

VII. The Basis Functions

Since the two-center Dirac Eq. (6.10) cannot be further separated and as no closed analytical solutions are at hand, the eigenvalue problem may be attacked in two ways: Either by numerical integration of (6.10) and imposing the proper matching conditions, or by diagonalization in a suitably chosen set of basis functions. We have chosen the latter one, because it facilitates the evaluation of matrix elements between states [69].

First, we need a complete set of basis functions. In generalization of the functions first given by Hylleraas [22] we take as spinor basis for the wave function $\psi(\xi, \eta)$ in Eq. (6.11):

$$\psi_{nls}^m(\xi, \eta) = e^{-x/2} L_n^{m+\varepsilon_s}(x) P_l^{m+\varepsilon_s}(\eta) \chi_s, \quad (7.1)$$

where we introduced a new variable

$$x = (\xi - 1)/a \quad (x \geqq 0) \quad (7.2)$$

and the spin-dependent parameter

$$\varepsilon_s = \begin{cases} -\tfrac{1}{2}, & s = 1, 3, \\ +\tfrac{1}{2}, & s = 2, 4. \end{cases} \quad (7.3)$$

The positive scaling parameter a in Eq. (7.2) will be determined further below [Equation (7.11)]. The exponential factor (7.1) accounts for the fact that we are dealing with bound state solutions which

asymptotically for $\xi \to \infty$ decay exponentially. The $L_n^\alpha(x)$ are the associated Laguerre polynomials defined by

$$L_n^\alpha(x) = \frac{\Gamma(n + \alpha + 1)}{\Gamma(\alpha + 1) \Gamma(n + 1)} \, {}_1F_1(-n, \alpha + 1; x) \quad (7.4)$$

and describe wave functions with asymptotically n radial nodes. The $P_l^\alpha(\eta)$ are the associated Legendre polynomials, and for the internuclear distance $2R$ approaching zero they go over into $P_l^\alpha(\cos \theta)$ of the one-center problem. Finally, the χ_s represent the four unit spinors with a one at the s-th place and all other components zero, i.e.

$$\sigma_z \chi_s = -\varepsilon_s \hbar \chi_s . \quad (7.5)$$

The indices n, l, s in (7.1) are defined on the set

$$\{(n, l, s) \mid n = 0, 1, 2, \dots; \quad (7.6)$$
$$l = m + \varepsilon_s, m + \varepsilon_s + 1, \dots; \quad s = 1, \dots, 4\}.$$

From mathematical arguments it is known [40] that the L_n^α and P_l^α form complete sets of orthogonal functions if n resp. l run over all allowed values (7.6). Therefore, the system (7.1) combined with the index set (7.6) forms a complete set of basis functions on the space

$$\{\xi \mid \xi \geqq 1\} \otimes \{\eta \mid -1 \leqq \eta \leqq 1\} \otimes \{s \mid s = 1, \dots, 4\}. \quad (7.7)$$

for square integrable wavefunctions.

We return to the scaling parameter a introduced in Equation (7.2). Asymptotically for $x \to \infty$ the basis functions (7.1) show the behavior

$$\psi_{nls}^m(\xi, \eta) \xrightarrow{x \to \infty} \exp\{-x/2\} \quad (7.8)$$

which has to be compared with the asymptotic behavior of bound states of the Dirac equation to a certain energy E:

$$\psi(|r|) \xrightarrow{|r| \to \infty} \exp\{-\sqrt{(m_e c^2)^2 - E^2} \, |r|/\hbar c\}. \quad (7.9)$$

In this formula it was assumed that the potential vanishes at infinity [41]. On the other hand, from (7.2) and (5.2) one has

$$x \to \xi/a \to |r|/R a \quad \text{for} \quad x \to \infty, \quad (7.10)$$

so that by comparison of (7.8) and (7.9) one finds

$$a = \frac{\hbar}{2 R m_e c} \left[1 - \left(\frac{E}{m_e c^2}\right)^2\right]^{-1/2}. \quad (7.11)$$

Thus a is determined by the energy of the bound state which is to be calculated.

In principle every arbitrary value of a could be chosen since the set (7.1) is complete for all values of a. In order to obtain rapid convergence of the numerical procedures applied, however, it is convenient to take such a value for a according to Eq. (7.11) with a good estimate of the expected energy E of the state under consideration. Then a has the same value for all the basis functions in (7.1). If one is interested in many bound states with very different energies at the same time, it is possible to take different values a_{nl} for the basis function ψ_{nls} according to the estimated energies E_{nls}.

To carry out the diagonalization of the Dirac Hamiltonian (6.10) in the basis (7.1) we need to know the matrix elements of the Hamiltonian with the basis functions. Writing (6.10) in the form

$$H_{\mathrm{TC}}\, \Psi = \Phi_m\, \tilde{H}^m_{\mathrm{TC}}\, \psi = E\, \Phi_m\, \psi \equiv E\, \Psi \quad (7.12)$$

one might be seduced to multiply with the operator Φ_m^{-1} from the left before taking matrix elements. This is possible because Φ_m is a regular matrix for all $\xi \neq 1$. However, this would complicate the diagonalization procedure, since Φ_m^{-1} and H_{TC} do not commute (this is the reason for $H_{\mathrm{TC}} \neq \tilde{H}^m_{\mathrm{TC}}$). It is well known that $B = A\,C$ is a hermitian operator, if and only if A and C are hermitian and commute with each other. Therefore $\tilde{H}^m_{\mathrm{TC}} \equiv \Phi_m^{-1}\, H_{\mathrm{TC}}\, \Phi_m$ is not a hermitian operator, and we have to take matrix elements of the full H_{TC}, i.e.

$$H_{\mathrm{TC}} = \Phi_m\, \tilde{H}^m_{\mathrm{TC}}\, \Phi_m^{-1} = \Phi_m \left[c\, \pi_m + \beta\, m_{\mathrm{e}}\, c^2 - \frac{e^2}{R} \frac{(Z_1 + Z_2)\xi - (Z_1 - Z_2)\eta}{\xi^2 - \eta^2} \right] \Phi_m^{-1} . \quad (7.13)$$

The matrix elements are

$$\langle \Psi^m_{n'l's'} | H_{\mathrm{TC}} | \Psi^m_{nls} \rangle = \langle \psi^m_{n'l's'} | \Phi_m^+ \Phi_m\, \tilde{H}^m_{\mathrm{TC}} | \psi^m_{nls} \rangle . \quad (7.14)$$

The right-hand side of the Dirac equation gives rise to the matrix elements

$$\langle \Psi^m_{n'l's'} | E | \Psi^m_{nls} \rangle = E\, \delta_{s's} \langle \psi^m_{n'l's'} | \Phi_m^+ \Phi_m | \psi^m_{nls} \rangle . \quad (7.15)$$

This matrix does not reduce to a diagonal unit matrix, because the basis functions (7.1) are not orthogonal due to the additional factor $\Phi_m^+ \Phi_m$ and the volume element in spheroidal coordinates $R^3 (\xi^2 - \eta^2)\, d\xi\, d\eta\, d\psi$.

Due to the simplicity and the suitable choice of the basis functions, all matrix elements (7.14) and (7.15) can be evaluated analytically. When the same scaling parameter a is used for all basis functions (7.1) the evaluation may be effected by reducing the matrix elements with help of recursive relations to the orthogonality relations for the polynomials $L_n^a(x)$ and $P_l^\alpha(\eta)$. This is shown in detail in Appendix B. On the other hand, when a variable scaling parameter a_{nl} is used, the matrix elements can be evaluated exactly with finite quadrature formulae for resulting integrals with exponentially decaying integrands. Since only polynomials enter, this method may be called analytic, too. Details for this integration scheme, which is better suited for numerical procedures than the resursive methods, are found in Appendix C.

By deliberate chosen scaling parameters a_{nl} the basis functions will not form a complete set. This is not very important in numerical calculations since the basis has to be truncated to finite dimensions, anyway. For theoretical considerations and coincidental convergence tests, however, one would prefer a constant scaling parameter for all basis functions, ensuring completeness in principle.

VIII. Extended Nuclear Charge Distributions

The importance of the finite nuclear radius becomes obvious when the electronic states in the field of one point nucleus are considered. When the central charge $Z e$ grows continuously, the binding energy of all bound states keeps increasing, until at $Z = \alpha^{-1} \approx 137.03602$ no eigenstates of angular momentum $j = 1/2$ exist [42]. Of course, the electrons occupying these states cannot disappear, if the nuclear charge grows beyond $137\,e$. In fact it can be shown that for nuclei with a finite charge distribution the bound states with $j = 1/2$ exist also for $Z\,a > 1$ [43, 5]. The actual binding energy is very sensitive to the nuclear radius ϱ.

There are immediate consequences for the two center problem. Even if every single nucleus is below the critical value $Z\,\alpha = 1$, it is possible that $(Z_1 + Z_2)\,a > 1$, e.g. $I + U$ gives $Z_1 + Z_2 = 145$ and experiments with similar systems have already been done [11]. As the internuclear distance $2\,R$ is shrinking to zero we obtain as limit just the disappearence of the $j = 1/2$ states, if the two nuclei are treated as pointlike. It has been shown earlier [41] that in this

case the binding energy of the deepest bound states grows beyond bound proportional to $1/R$, i.e. diverges for $R \to 0$. Notwithstanding this divergence for small internuclear separations, the discrepancy between states of pointlike and those of extended nuclei will be large. Therefore we are compelled to replace — at least for very heavy systems and small separations — the $1/r$-Coulomb potential by the potential of finite charge distributions.

In general it is impossible to evaluate the matrix element with a cut-off Coulomb potential analytically. In order to keep the numerical computations small, we proceed as follows: Denoting the exact $1/r$-potentials by V_c and that of extended nuclei by V_{ex}, we may write

$$V_{ex}(r_1, r_2) = V_c(r_1, r_2) + [V_{ex}(r_1, r_2) - V_c(r_1, r_2)] . \tag{8.1}$$

The term in brackets vanishes everywhere, except inside the two nuclear volumes, if the nuclei are spherical:

$$\{(r_1, r_2) \,|\, r_1 \leqq \varrho_1 \quad \text{or} \quad r_2 \leqq \varrho_2\} . \tag{8.2}$$

ϱ_1 and ϱ_2 are the two nuclear radii. The matrix elements

$$\langle \Psi^m_{n'l's} | V_c(r_1, r_2) | \Psi^m_{nls} \rangle \tag{8.3}$$

are known analytically from the considerations in Chapter VII.

It only remains to evaluate

$$\langle \Psi^m_{n'l's} | V_{ex}(r_1, r_2) - V_c(r_1, r_2) | \Psi^m_{nls} \rangle . \tag{8.4}$$

The potentials of the two nuclei superpose linearly — as long as the nuclei do not overlap — and we may restrict ourselves to point out the method for one nucleus. The nuclear radius be ϱ_1. Then for $r_1 \leqq \varrho_1$ we have

$$V_{ex}(r_1, r_2) - V_c(r_1, r_2) = V_{N_1}(r_1) + Z_1 e^2/r_1 \tag{8.5}$$

$$= \frac{Z_1 e^2}{R} \left[v_{N_1}[R(\xi + \eta)] + \frac{1}{\xi + \eta} \right]$$

where $V_{N_1} = (Z_1 e^2/R) v_{N_1}$ was used. Introducing $\beta_1 = \varrho_1/R$, the nuclear volume is defined in spheroidal coordinates

$$\{(r_1, r_2) \,|\, r_1 \leqq \varrho_1\} = \{(\xi, \eta) \,|\, 1 \leqq \xi \leqq \beta_1 - \eta \quad \text{and} \quad -1 \leqq \eta \leqq -1 + \beta_1\} . \tag{8.6}$$

With the basis functions ψ^m_{nls} from Eq. (7.1) the matrix element (8.4) becomes

$$2 \pi R^2 Z_1 e^2 \int_{-1}^{-1+\beta_1} d\eta \int_{1}^{\beta_1 - \eta} d\xi (\xi^2 - \eta^2)(\xi^2 - 1)^{m + \varepsilon_s} \cdot \exp\left\{-\tfrac{1}{2}(x_{n'l'} + x_{nl})\right\} \cdot L^{m+\varepsilon_s}_{n'}(x_{n'l'}) L^{m+\varepsilon_s}_n(x_{nl}) \tag{8.7}$$

$$\cdot P^{m+\varepsilon_s}_{l'}(\eta) P^{m+\varepsilon_s}_l(\eta) \left[v_{N_1}(R(\xi + \eta)) + \frac{1}{\xi + \eta} \right] .$$

We have used the symbol ε_s (7.3) and accounted for the possibility to employ variable scaling parameters a_{nl}. The simplest choice is that of a homogeneous charge distribution inside the spherical nuclei, which leads to

$$v_{N_1}(r_1) = -\frac{R}{2 \varrho_1} \left[3 - \left(\frac{r_1}{\varrho_1}\right)^2 \right] . \tag{8.8}$$

This potential (8.8) has been applied in all our calculations where the finiteness of the nuclei was taken into account.

IX. Numerical Procedures

Any numerical method for the solution of the matrix form of the twocentre Dirac equation begins with cutting off the basis and reducing the involved matrices to finite dimensions. Before investigating the convergence of this procedure we give the method employed for carrying out the search for eigenvalues and eigenstates of the matrix equation.

$$H \,|\, \psi \rangle = E N \,|\, \psi \rangle \tag{9.1}$$

where H is the matrix of the Hamiltonian and N the non-diagonal normalization matrix of the scalar products of the basis functions. N could be made diagonal by first orthogonalizing the basis functions with the method given by Schmidt. It is, however, more convenient to keep the non-orthogonal basis and solve the problem by first diagonalizing N and then H.

We proceed as follows: N is certainly hermitian, since it is the matrix of scalar products. Therefore, we can find a unitary transformation U, such that $U N U^+ = N'$ is diagonal with only real elements:

$$H' \,|\, \psi' \rangle = (U H U^+) U \,|\, \psi \rangle = E (U N U^+) U \,|\, \psi \rangle$$
$$= E N' \,|\, \psi' \rangle . \tag{9.2}$$

H', N' and $|\, \psi' \rangle$ are the matrices and vectors after transformation. Because the scalar product is by definition positive definite, N' has only positive elements. Therefore there is a diagonal, positive real matrix S, such that

$$S S = N' ,$$

and S is regular (our basis is linearly independent). Then the inverse matrices N'^{-1} and S^{-1} exist and from (9.2) becomes

$$S^{-1} H' S^{-1} S \,|\, \psi' \rangle = E \, S^{-1} N' S^{-1} S \,|\, \psi' \rangle . \quad (9.3)$$

S^{-1} and N commute being diagonal and with

$$H'' = S^{-1} H' S^{-1} = S (N^{-1} H') S^{-1} , \\ |\, \psi'' \rangle = S \,|\, \psi' \rangle \quad \left. \right\} \quad (9.4)$$

we are left with an eigenvalue problem involving only one matrix

$$H'' \,|\, \psi'' \rangle = E \,|\, \psi'' \rangle . \quad (9.5)$$

Since H and H' are hermitian, so is H'':

$$(H'')^+ = (S^{-1} H' S^{-1})^+ = S^{-1+} H'^+ S^{-1+} \\ = S^{-1} H' S^{-1} = H'' , \quad (9.6)$$

because S^{-1} is diagonal with only real elements.

Now one can find a unitary transformation V diagonalizing H'':

$$H''' \,|\, \psi''' \rangle = V H'' V^+ V \,|\, \psi'' \rangle \\ = E V \,|\, \psi'' \rangle = E \,|\, \psi''' \rangle . \quad (9.7)$$

Altogether we have

$$H''' = V S^{-1} U H U^+ S^{-1} V^+ \\ = V S U (N^{-1} H) U^+ S^{-1} V^+ , \quad \left. \right\} \quad (9.8\,\text{a})$$

$$|\, \psi''' \rangle = V S U \,|\, \psi \rangle \quad (9.8\,\text{b})$$

and H''' contains in the diagonal the eigenvalues of the two-centre Hamiltonian.

The matrix S plays the role of a non-orthogonal transformation required to pass from the non-orthogonal basis functions to the necessarily orthogonal eigenstates. U and V are additional rotations.
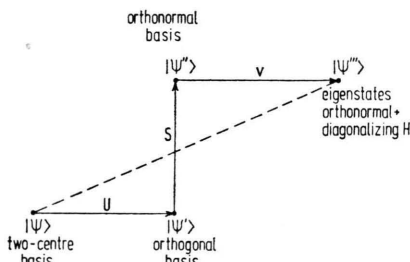
Fig. 2. Schematic explanation of the diagonalization procedure employed. Three steps are involved to obtain the eigenstates in the non-orthogonal two centres basis.

The two numerical diagonalizations required for the method sketched above were carried out by a subroutine utilizing the Jacobian method [44], with an accuracy of 1 part in 10^6. Most computations were performed in a basis containing 100 vectors. This usually assured satisfactory convergence. In the united atom limit the accuracy was of the order of 0.1 per cent, deteriorating for growing internuclear separation. On the Frankfurt Univac 1108 the computation of the matrix elements took $4 - 8$ seconds, the subsequent diagonalization $90 - 200$ seconds, depending on the special molecular system.

X. General Features of the Level Diagrams

a) Symmetric Systems

Molecules with two nuclei of the same charge show energetically degenerate states belonging to the two identical separate atoms at infinitely large separations. During the approach of the two centres all states are lowered by $- Z e^2 / R$ in energy, which corresponds to the expectation value of the perturbing potential in first order. When the separation distance becomes comparable in size to the dimensions of an atomic state under consideration, the state is polarized. This transition is smooth, of course.

If there are several degenerate states, any interaction will spread them in energy. In the relativistic case this is true for states of same total angular momentum j, e.g. $2s_{1/2}$ and $2p_{1/2}$. The interaction between them is up to first order (a_0 is the Bohr radius)

$$\Delta E = (Z e^2 / R^2) \langle 2s_{1/2} |\, r Y_{10} \,|\, 2p_{1/2} \rangle \approx \sqrt{3} (e^2 / R) a_0 . \quad (10.1)$$

This is the same as for the linear Stark effect of atoms in a static electric field. For light systems, the $2p_{1/2} - 2p_{3/2}$ fine structure splitting is much smaller than the interaction due to the second Coulomb centre. In this case it may be regarded as degenerate, too, and one retains the nonrelativistic size of the linear Stark effect

$$\Delta E_{nr} = 3 (e^2 / R^2) a_0 . \quad (10.2)$$

In general, the following picture is valid:

The operators J_z and βP, i.e. axial angular momentum and parity, commute with the Hamiltonian. All molecular states exhibit good parity and good angular momentum around the axis through the two centres. States of different quantum numbers $m = \langle J_z \rangle$ or of opposite parity cross without interaction. States that do not differ in one of these

quantum numbers must not cross (for details see Section XI).

The commonly accepted nomenclature for the molecular states makes use of the quantum numbers that are assumed in the united atoms limit $R \to 0$, besides the magnetic quantum number m and parity (g = gerade = even, u = ungerade = odd). The lowest molecular state is always the $1s_{1/2}\sigma_g$ state, above it the $2\,p_{1/2}\,\sigma_u$ state. For $R \to \infty$ these two states are degenerate, they pass over into the symmetric and antimetric superposition of the two 1 s-states of the individual atoms, respectively. As the $2\,p_{1/2}$-state is below the $2s_{1/2}$-state when the nucleus is treated as finite, these two molecular states never have crossings with other states.

The molecular states with high angular momentum, i.e. the d- and f-states, are in general lowered in energy when the two centres approach, but already at fairly large distances they rise again steeply so that they may be bound even weaker in the compound system than in the separated atoms. This phenomenon leads to the idea of promotion of molecular states[1], which is of importance for the qualitative explanation of reaction cross sections.

b) Asymmetric Systems

Asymmetric molecular systems differ from symmetric ones in principle by the lack of parity conservation. Consequently, the molecular states can only be classified according to their axial angular momentum m, and only states with different m are allowed to cross.

For simplicity we assume $Z_1 > Z_2$. The only general feature of all asymmetric systems is that the lowest molecular state $1s_{1/2}\sigma$ ends up in the $1s_{1/2}$ state of the heavier partner. The scheme of the higher molecular states depends upon the ratio $Z_1 : Z_2$. If this ratio is smaller than $2\sqrt{1 - Z_2^2\,\alpha^2} : 1$ the 1 s-state in the Z_2 atom is stronger bound than the $2p_{1/2}$-state in the Z_1 atom. (For light molecules the ratio is just $2 : 1$.) Then the $2\,p_{1/2}\,\sigma$-state, i.e. the second lowest molecular level, ends up in the 1 s-state of the lighter partner. Otherwise, for $Z_1 : Z_2 > 2\sqrt{1 - Z_2^2\,\alpha^2} : 1$ the molecular $2\,p_{1/2}\,\sigma$ level connects the $2p_{1/2}$-states of the compound system and the heavier partner atom.

It is clear that the level scheme for the higher states of the intermediate molecule allows for a great number of possible combinations according to the ratio $Z_1 : Z_2$. A qualitative scheme can be constructed in every case from the following arguments[45]: (1) The axial angular momentum is conserved; (2) the molecular states tend to connect states with the same number of radial nodes in the two asymptotic limits $R \to 0$ and $R \to \infty$; (3) states with the same symmetry are not allowed to cross.

It is obvious that the rule (2) has to be given up when (3) applies, i.e. when an adiabatic level suddenly changes its configuration. The level schemes which are obtained by obeying prescription (2) even if the noncrossing rule has to be violated are called diabatic. A sophisticated theoretical justification for this point of view was attempted by Smith[3].

An interesting phenomenon occurring in slightly asymmetric systems $(Z_1 : Z_2 \approx 1)$ should be mentioned. Upon approach of the two Coulomb centres the K-shell of the heavier partner is lowered by $-Z_2 e^2/R$ in energy, whereas the K-shell of the lighter partner is lowered by $-Z_1 e^2/R$, i.e. a greater amount. Therefore the two molecular orbitals $1\,s\,\sigma$ and $2p_{1/2}\,\sigma$ approach each other when R is decreased. As soon as R becomes comparable to the K-shell radius, first order perturbation theory fails, higher order terms become important and the separation energy between the two states grows again. This pseudocrossing will be further discussed in Section XI.

XI. Level Crossings

The most interesting features of two centre level diagrams occur at the crossing point of two molecular states or at points where they approach each other very closely. The well-known anti-crossing rule of Neumann and Wigner[46] states that in general it is impossible to reach the coincidence of two energy eigenvalues by variation of one real parameter: More precisely, one needs at least two real parameters when the Hamiltonian is real and three whenever it is complex hermitian. "In general" means that it is only valid for states with the same symmetry properties.

In the nonrelativistic two centre Coulomb problem an additional constant of motion exists, so that the v. Neumann-Wigner rule is inapplicable. The molecular states can cross as they like[35, 36, 47]. In Sect. IV we have seen that this is not the case for the relativistic problem, therefore the non-crossing rule applies. In Sect. X it has already been mentioned that crossings are allowed for states with different $\langle J_z \rangle = m$ and, in the case of symmetric molecules, for states of opposite parity.

However, it is worthwhile to investigate two practical examples. One is the avoided crossing of two σ-levels of the same parity in the molecule Br − Br. We select the $2\,s_{1/2}\,\sigma$ and the $3\,d_{3/2}\,\sigma$ states which approach at about 7500 fm internuclear distance (see Fig. 14). Figure 3 shows on a large scale the
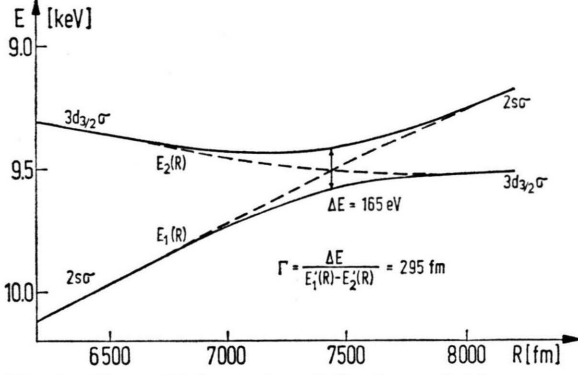

Fig. 3. The avoided crossing of the $2s\sigma$ and $3d_{3/2}\sigma$ states in the Br+Br quasimolecule at $R=7450$ fm. The repulsion between the two molecular levels is a purely relativistic effect.

region between 6200 fm and 8200 fm distance. The crossing is actually avoided. Remembering that this does not occur for the corresponding non-relativistic states the repulsion must be due to one of the relativistic corrections *. These are [48] the Darwin term

$$W_1 = \frac{1}{8}\left(\frac{\hbar}{m\,c}\right) \Delta V(\mathbf{r}) = \frac{1}{8}\left(\frac{\hbar\,e}{m\,c}\right)^2$$
$$\times \left(\frac{Z_1}{r_1^{\,2}}\,\delta(\mathbf{r}_1) + \frac{Z_2}{r_2^{\,2}}\,\delta(\mathbf{r}_2)\right), \qquad (11.1)$$

the relativistic contribution to the kinetic energy

$$W_2 = -\frac{[E - m\,c^2 - V(\mathbf{r})]^2}{2\,m\,c^2}$$
$$= -\frac{(E - m\,c^2)^2}{2\,m\,c^2} - \frac{(E - m\,c^2)}{m\,c^2}\left(\frac{Z_1\,e^2}{r_1} + \frac{Z_2\,e^2}{r_2}\right)$$
$$- \frac{e^4}{2\,m\,c^2}\left(\frac{Z_1}{r_1} + \frac{Z_2}{r_2}\right)^2 \qquad (11.2)$$

and finally the spin-orbit coupling

$$W_3 = \frac{\hbar\,\boldsymbol{\sigma}}{4\,m^2\,c^2} \cdot [(\operatorname{grad} V(\mathbf{r})) \times \boldsymbol{p}]$$
$$= \frac{e^2\,\hbar\,\boldsymbol{\sigma}}{4\,m^2\,c^2} \cdot \left[\frac{Z_1}{r_1^{\,3}}\,\boldsymbol{L}_1 + \frac{Z_2}{r_2^{\,3}}\,\boldsymbol{L}_2\right]. \qquad (11.3)$$

Unfortunately, all three interactions contribute to the repulsion of the levels, since both (11.1) and

---

* Also, for very heavy systems, the finite nuclear extension has an effect in this direction.

(11.3) as well as the third term in (11.2) do not belong to the class of separable (non-relativistic) two-centre potentials that were given in Equation (4.4).

Moreover, they are of the same order of magnitude (250 eV) for the states under consideration, viz. the 2 s σ and the 3 $d_{3/2}$ σ state.

Our numerical finding proves again that the Dirac equation cannot be separable for a two-center potential (see also Chapter IV). Comparing the repulsion of the two states with their energy slope we find that the change of the symmetry of the states happens within

$$\Gamma = \frac{\Delta E}{\dfrac{\partial}{\partial R}\,[E_1(R) - E_2(R)]} \approx 295\;\text{fm}. \qquad (11.4)$$

Instead of the binding energy we could look at the symmetry properties of the two wave functions. Within the short range of the avoided crossing the two states can be represented by

$$|1\rangle = \sin\varphi\,|2s\sigma\rangle + \cos\varphi\,|3d\sigma\rangle,$$
$$|2\rangle = \cos\varphi\,|2s\sigma\rangle - \sin\varphi\,|3d\sigma\rangle \qquad (11.5)$$

with φ being a function of R. $|2\,s\,\sigma\rangle$ and $|3\,d\,\sigma\rangle$ denote not the exact eigenfunctions of the adiabatic Hamiltonian but the wave functions with unchanged symmetry as it is before the crossing (i.e. the diabatic wave functions). φ varies between 0 and $\pi/2$ when R runs over the crossing. This phase change of $\pi/2$ is characteristic for such an avoided crossing.

The numerically calculated phase $\varphi(R)$ is shown in Figure 4. The center of the phase change is at 7450 fm and the width (change of φ by $\pi/4$) is
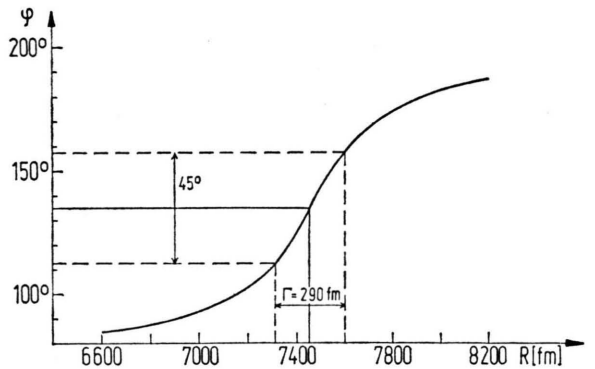

Fig. 4. The mixing phase between the adiabatic $2s\sigma$ and $3d_{3/2}s$ states in Br+Br as a function of the internuclear separation R (cf. Figure 3). The total phase change is 90°. Diabatic states are obtained by inverting the rotation.

290 fm, again. This confirms the results from the energy diagram.

Most avoided crossings in two center diagrams are of the same type as the $2\,\mathrm{s}\,\sigma - 3\,\mathrm{d}_{3/2}\,\sigma$ pseudo-crossing in Br − Br. In slightly asymmetric systems, however, a completely different phenomenon is observed. Figure 5 shows that the $2\,\mathrm{p}_{1/2}\,\sigma$ and the $1\,\mathrm{s}\,\sigma$ molecular states in Br − Zr $(Z_1 = 35,\ Z_2 = 4)$ approach at an internuclear distance $R \approx 10^4$ fm. They do not cross but are repelled, which is in accordance with the system being asymmetric and the states having no good parity. That this comes about because the heavier charge is acting on the lighter atom and vice versa was already explained in Section X (6).

In contrast to what we had for a pseudo-crossing in a symmetric system [see Eq. (11.5)] with the mixture phase φ varying between 0 and $\pi/2$, we now have on the one side of the pseudo-crossing

$$|1\rangle = |1\mathrm{s}\sigma\rangle,\quad |2\rangle = |2\mathrm{p}_{1/2}\sigma\rangle \qquad (11.6)$$

and on the other side

$$|1\rangle = \frac{1}{\sqrt{2}}\left(|1\mathrm{s}\sigma\rangle + |2\mathrm{p}_{1/2}\sigma\rangle\right),$$
$$|2\rangle = \frac{1}{\sqrt{2}}\left(|1\mathrm{s}\sigma\rangle - |2\mathrm{p}_{1/2}\sigma\rangle\right). \qquad (11.7)$$

This can be expressed by the Eq. (11.5) but the phase φ varies between 0 and $\pi/2$. The cause for this behaviour can be seen as follows: When R increases, Fig. 5 shows two states $|1\mathrm{s}\,\sigma\rangle$ and $|2\,\mathrm{p}_{1/2}\,\sigma\rangle$ of about good, but opposite parity, since in the system Br + Zr we still have $(Z_1 - Z_2) \ll Z_1 + Z_2$. As R increases up to a distance of about $R = 10^4$ fm the recoupling to the two atomic K-states of Br and
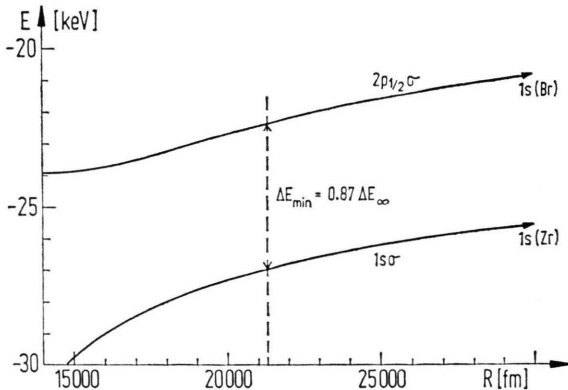
Zr takes place. These are essentially sum and difference of the two molecular states we started with. (The argument is only exact in symmetrical systems, but there the two K-shells are degenerate and every linear combination is an eigenstate. Only the parity-nonconserving part of the interaction in asymmetric molecules forces to the recoupling of states.)

In a perturbation theory approach, one can show that the energies of the $1\,\mathrm{s}\,\sigma$ and $2\,\mathrm{p}_{1/2}\,\sigma$ states will be

$$E_{1/2} = E_\infty - \frac{Z\,e^2}{R} \pm \left[\left(\frac{Z_1 - Z_2}{Z}\right)^2 \left(E_\infty + \frac{Z\,e^2}{R}\right)^2 \right.$$
$$\left. + \left(1 + \frac{R}{a} + \frac{R^2}{3\,a}\right)^2 \exp\left\{-\frac{2\,R}{a}\right\}\left(E_\infty - \frac{Z\,e^2}{R}\right)^2\right]^{1/2}$$
$$(11.8)$$

with $Z = \frac{1}{2}(Z_1 + Z_2)$ and $a = \hbar^2/Z\,e^2\,m$ being the Bohr radius of the Z atomic K-shell, $E_\infty < 0$ being its binding energy. The difference $E_1 - E_2$ is easily seem to have a minimum when the exponential term begins to balance the potential term in the square root. Numerical evaluation of (11.8) indicates that this minimum is attained at $R \sim 15\,a$ and is 10 to 15 percent lower than the separation of the K-shells in the single atoms. The relative effect is larger with $\Delta Z/Z$ and happens at smaller separation distances.

XII. Spin-Orbit-Interaction for $R \to 0$

In the limit of vanishing internuclear distance R the molecular states of the two centre Dirac equation become atomic states with good total angular momentum j^2. All electronic states with an orbital angular momentum higher than zero, i.e. p, d, f, etc. states, are split up into a $j = l - \frac{1}{2}$ and a $j = l + \frac{1}{2}$ states. This splitting is due to the spinorbit interaction W_3 (11.3).

When the two nuclei are torn apart the potential becomes a two centres potential which deviates from the strictly atomic potential by the admixture of angle dependent terms (we assume a symmetric system):

$$-\frac{Z\,e^2}{2\,|\boldsymbol{r} - \boldsymbol{R}|} - \frac{Z\,e^2}{2\,|\boldsymbol{r} + \boldsymbol{R}|}$$
$$= -Z\,e^2 \sum_{l=0}^{\infty} \frac{R^{2l}}{r^{2l+1}}\,P_{2l}(\cos\vartheta). \qquad (12.1)$$

This expansion is valid in the region $r \geq R$. The lowest order correction to the atomic potential is therefore a quadrupole interaction

$$H_{\mathrm{QP}} = -Z\,e^2 (R^2/r^3)\,P_2(\cos\vartheta). \qquad (12.2)$$

Fig. 5. The pseudocrossing of the $1\mathrm{s}\sigma$ and $2\mathrm{p}_{1/2}\sigma$ states in Br + Zr. The repulsive interaction is nonrelativistic in origin and very large compared to the one acting in Figure 3.

We now want to investigate the effect of this potential on atomic wave functions with spin j

$$|\psi_j^\mu\rangle = f_l(r) \sum_m (l\,\tfrac{1}{2}\,j\,|\,\mu - m\,m\,\mu)\, Y_l^{\mu-m}\, \chi^m \quad (12.3)$$

which are eigenstates to a Hamiltonian with spin-orbit coupling $H = H_0 + H_{\mathrm{so}}$. If we have two states $|\psi_{l-1/2}^\mu\rangle$ and $|\psi_{l+1/2}^\mu\rangle$, they are initially separated by [49]

$$E_{l+\frac{1}{2}}^0 - E_{l-\frac{1}{2}}^0 = a\,(l+\tfrac{1}{2}) \quad (12.4)$$

where a is an abbreviation for

$$a = \frac{(Z\,\alpha)^4}{2\,n^3\,l(l+1)\,(l+\frac{1}{2})}\, m\,c^2. \quad (12.5)$$

The matrix elements of H_{QP} with these wave functions are

$$\langle \psi_j^\mu | H_{\mathrm{QP}} | \psi_j^\mu \rangle = -2\,a\left(\frac{R\,m\,c}{\hbar}\right)^2$$
$$\times \frac{(2\,l+1)\,[l(l+1)-3(\mu^2+\frac{1}{4})]+12\,(j-l)\,\mu^2}{(2\,l+3)\,(2\,l+1)\,(2\,l-1)}, \quad (12.6)$$

$$\langle \psi_{l-\frac{1}{2}}^\mu | H_{\mathrm{QP}} | \psi_{l+\frac{1}{2}}^\mu \rangle = 4\,a\left(\frac{R\,m\,c}{\hbar}\right)^2$$
$$\times \frac{3\,\mu\,\sqrt{(l+\frac{1}{2})^2-\mu^2}}{(2\,l+3)\,(2\,l+1)\,(2\,l-1)}. \quad (12.7)$$

For an illustration we choose the 2 p wave functions

$$|1\rangle = |\,2\,\mathrm{p}_{1/2,\,1/2}\rangle, \quad |2\rangle = |\,2\,\mathrm{p}_{3/2,\,1/2}\rangle$$
$$\text{and} \quad |3\rangle = |\,2\,\mathrm{p}_{3/2,\,3/2}\rangle.$$

For these Eqs. (12.6 and 7) yield:

$$\left.\begin{array}{l} (H_{\mathrm{QP}})_{11} = 0, \\ (H_{\mathrm{QP}})_{22} = -\tfrac{2}{5}\,a\,(R\,m\,c/\hbar)^2, \\ (H_{\mathrm{QP}})_{33} = \tfrac{2}{5}\,a\,(R\,m\,c/\hbar)^2, \end{array}\right\} \quad (12.8)$$

and the only non-vanishing interaction is

$$(H_{\mathrm{QP}})_{12} = \pm\,\frac{2\,\sqrt{2}}{5}\,a\left(\frac{R\,m\,c}{\hbar}\right)^2. \quad (12.9)$$

Perturbation theory for two nearly degenerate states [50] gives as eigenstates to the Hamiltonian $H = H_0 + H_{\mathrm{SP}} + H_{\mathrm{QP}}$:

$$E_{1,2} = \tfrac{1}{2}\,[E_{l+\frac{1}{2}}^0 + E_{l-\frac{1}{2}}^0 + (H_{\mathrm{QP}})_{11} + (H_{\mathrm{QP}})_{22}]$$
$$\pm \{\tfrac{1}{4}\,[E_{l+\frac{1}{2}}^0 - E_{l-\frac{1}{2}}^0 + (H_{\mathrm{QP}})_{22} - (H_{\mathrm{QP}})_{11}]^2$$
$$+ (H_{\mathrm{QP}})_{12}{}^2\}^{1/2}. \quad (12.10)$$

This gives for the 2 p-states

$$E_{1,2} = E^0 - \frac{a}{4} - \frac{1}{5}\,a\,\varrho^2 \pm \frac{3}{5}\,a\,\varrho^2$$
$$\times \sqrt{1 - \frac{5}{6\,\varrho^2} + \frac{25}{16\,\varrho^4}} \quad (12.11)$$

where $E^0 = [-(Z\,\alpha)^2/2\,n^2]\,m_e\,c^2$ is the (non-relativistic) energy of the n p-states without spin, and $\varrho = R\,m\,c/\hbar$. An expansion for $\varrho \gg 1$ yields

$$\left.\begin{array}{l} E_1 = E^0 \qquad\qquad - \dfrac{4}{5}\,a\,\varrho^2, \\[2mm] E_2 = \left(E^0 - \dfrac{a}{2}\right) + \dfrac{2}{5}\,a\,\varrho^2, \end{array}\right\} \quad (12.12)$$

and for the π-state simply

$$E_3 = \left(E^0 + \frac{a}{2}\right) + \frac{2}{5}\,a\,\varrho^2. \quad (12.13)$$

The corresponding wave functions are determined by [55]

$$\left.\begin{array}{l} |\psi_1\rangle = |\psi_{l-1/2}\rangle \cos\beta + |\psi_{l+1/2}\rangle \sin\beta, \\ |\psi_2\rangle = -|\psi_{l-1/2}\rangle \sin\beta + |\psi_{l+1/2}\rangle \sin\beta, \end{array}\right\} \quad (12.14)$$

with

$$\tan 2\beta = 2\,(H_{\mathrm{QP}})_{12}/[(H_{\mathrm{QP}})_{11} - (H_{\mathrm{QP}})_{22}]. \quad (12.15)$$

The two limits show that the wave functions, which are initially states of good total angular momentum $j^2\,(\varrho \ll 1)$:

$$|\psi_1\rangle = |2\mathrm{p}_{1/2,1/2}\rangle, \quad |\psi_2\rangle = |2\mathrm{p}_{3/2,1/2}\rangle \quad (12.16)$$

are decoupled in the spin components by the quadrupole interaction and for $\varrho \gg 1$ one has wave functions to good l^2 and s^2:

$$|\psi_1\rangle = |2\mathrm{p}\sigma\rangle, \quad |\psi_2\rangle = |2\mathrm{p}\pi\downarrow\rangle. \quad (12.17)$$

This behaviour is illustrated in Fig. 6, where the eigenstates in perturbation theory and the asymptotic states for $\varrho \ll 1$ and $\varrho \gg 1$ are drawn. The transition between the regions where spin-orbit interaction resp. quadrupole interaction dominates is independent of the system at the Compton wavelength of the electron. In Fig. 7 we show how the wave functions change from those of good j^2 to those of good l^2 due to the change from a one-centre to a two centres potential.

For asymmetric systems one also has to take into account a dipole interaction term in Eq. (12.1) and the 2 p states couple to the 2 s state in addition.
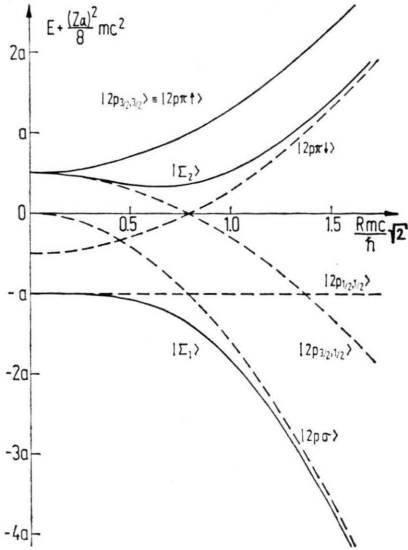
Fig. 6. The spin-orbit angular momentum recoupling for the 2p molecular states at small internuclear separations. For symmetric systems no coupling to the 2sσ level occurs. The internuclear separation scale is independent (to lowest order) of the system involved.
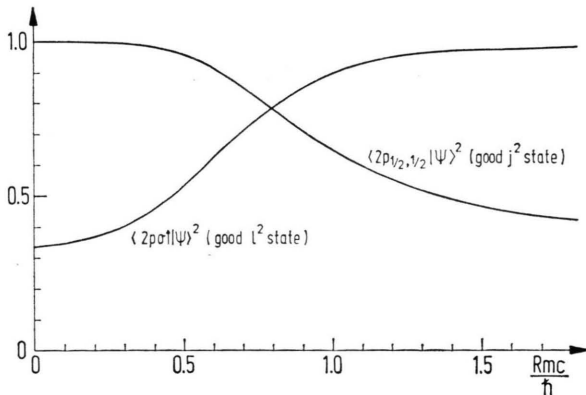

Fig. 7. The contributions of the various good j^2 resp. good l^2 atomic states to the lowest one of the 2p molecular states in the angular momentum recoupling region. For small separations R the state is an eigenstate of the total angular momentum whereas for large R it becomes eigenstates of good orbital angular momentum.

XIII. Critical Distance

The discrepancy between the solutions of the relativistic and the non-relativistic wave equation becomes more and more qualitative when the electrons are very strongly bound. This is most obvious if $(Z_1 + Z_2) a > 1$. For a point charge $Z a > 1$ the Dirac equation does not yield any bound $j = 1/2$

states. If the nucleus is divided into two parts Z_1 and Z_2, this singularity disappears for every finite distance R between the fragments. However, when $R \to 0$ the binding energy of each $j = 1/2$ state increases beyond bound as R^{-1} (see Ref. 40).

It has been explained before (Sect. VIII) that in this so-called over-critical case a point charge is an unallowed idealization of the physical nucleus. We have assumed a spherical constant charge distribution inside the nuclei which leads to a harmonic oscillator cut-off of the Coulomb potential (8.8).
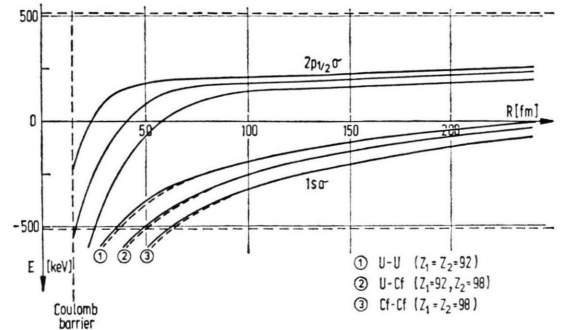
Fig. 8. The "diving" molecular states for the system U+U (1), U+Cf (2) and Cf+Cf (3). For the 1sσ levels the point nucleus solutions are indicated by broken lines. In the region of interest the differences are small.

Figure 8 shows the two lowest molecular states 1 s σ and 2 $p_{1/2}$ σ for three over-critical systems (U − U, U − Cf, Cf − Cf). The states have only been calculated down to the Coulomb barrier ($R = 15$ fm), since upon further approach the two nuclei overlap and the nuclear wave functions will change. The charge distribution then becomes time-dependent as a function of scattering energy and compression modes have to be taken into account [51].

The critical distance R_{cr}, where the binding energy of a state equals $2 m_e c^2$, is of vital importance for the positron autoionization cross-sections in heavy ion collisions [19]. The precise values of R_{cr} for homogeneously charged nuclei with radius $r_0 = 1.2$ fm $\cdot A^{1/3}$ are contained in the following table:

	$R_{cr}(1s\sigma)$	$R_{cr}(2p_{1/2}\sigma)$
U−U	34.7 fm	—
U−Cf	47.7 fm	16.1 fm
Cf−Cf	61.1 fm	25.4 fm

Due to non-adiabatic effects the 2 $p_{1/2}$ σ level plays also a role in positron creation even if it does not

completely reach the negative energy continuum, as e.g. in U − U (see Ref. 52).

In Table 1 we present the wave function 1 s σ of the U + U system at the critical internuclear distance. The $n = l = 0$, $s = 1$ component is dominating, which fact ensures good convergence of the basis set.

n	l	s	$R = 34$ fm
0			.53854
1			−.27449
2	0		.14959
3			−.09271
4			.09278
0			−.02144
1			−.00398
2	2	1	−.00026
3			−.00314
4			.00930
0			−.00683
1			−.02217
2	4		.03615
3			−.07767
4			−.01805
0			.02143
1			.00948
2	2		.00269
3			.01700
4		2	−.01611
0			.00223
1			−.02375
2	4		.05071
3			−.04967
4			−.04494
Energy (keV)			−1026,7

Table 1. The 1sσ wave function at the critical distance $R = 34$ fm for the quasi-molecular system U+U. All nonvanishing components are given.

XIV. Level Diagrams

So far we have discussed the theoretical details of the relativistic two centre problems and given a procedure to solve for the electronic bound states. In this section we present some numerical results for selected molecular systems. For light systems $(Z_1, Z_2 < 20)$ the relativistic corrections to the binding energies are very small. Since there is no hope that inner-shell molecular systems can be studied for more than 10^{-12} sec in ion-atom collisions, there is an inherent experimental uncertainty of $10 - 100$ eV to any such state. This covers up all relativistic effects except spin-orbit coupling[53].

The lightest system we study, Ni + Ni, is of interest in molecular K-radiation measured by Greenberg et al.[15] (Figures 9 − 11). The general features of this symmetric system have been discussed in Section X a. The overall level scheme (Fig. 9) shows a
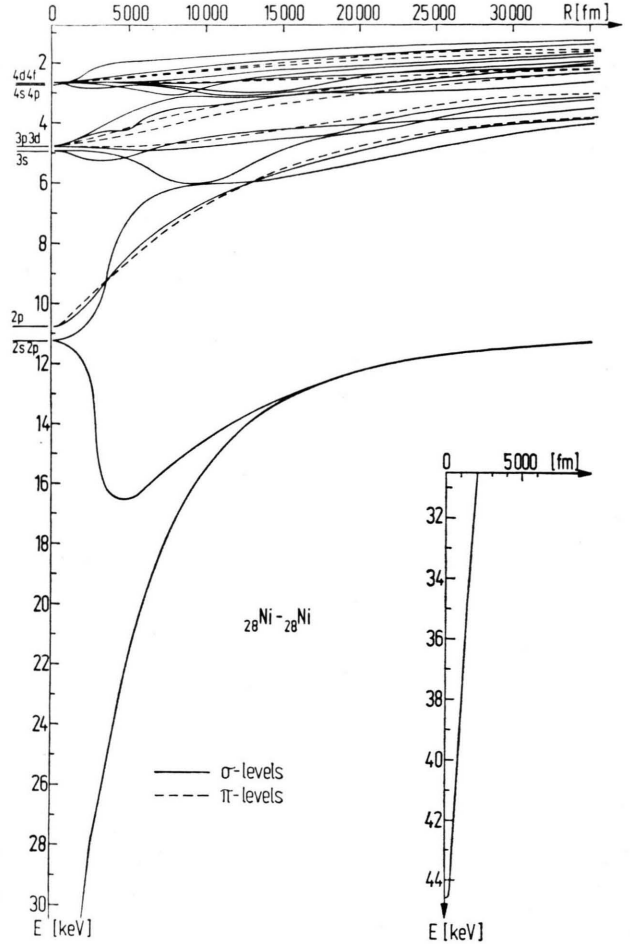
Fig. 9. The σ- and π-molecular levels of the Ni+Ni, $(Z_1 = Z_2 = 28)$ system in double logarithmic scale.

typical rearrangement region for the higher molecular states in the region $10^4 - 2 \times 10^4$ fm, which is shown in detail on a linear scale in Fig. 10. Characteristic are steeply moving states and many allowed and forbidden crossing points. At high collision velocities $(E_{lab} \gg 1 \text{ MeV})$ it can be expected that diabatic states would give a more physical description of this region. They can be constructed from the adiabatic states using a unitary transformation, viz. the inverse rotation given in Eq. (11.5) (see Ref. 54). So, although the adiabatic states may not have great physical significance, they may serve as a practical basis to construct diabatic states. From $R \sim 10^4$ fm down to $R \sim 10^2$ fm the newly formed molecular states approach energetically their united atom limit. Typically one then has a long $(\sim 1000$ fm) "runway" during which the energies
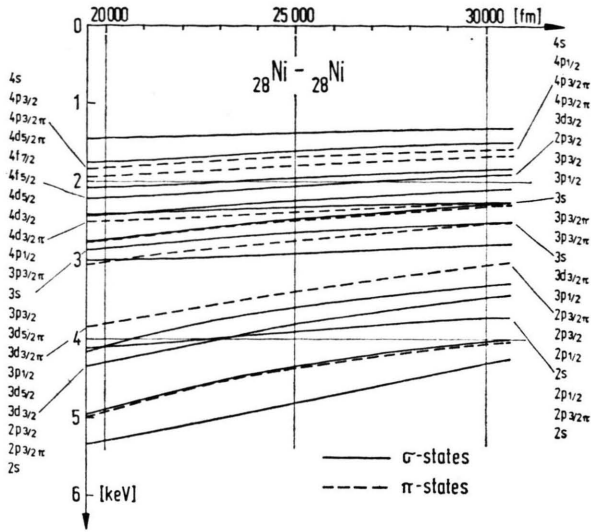
Fig. 10. The rearrangement region in the Ni+Ni quasi-molecule. The scale is linear.
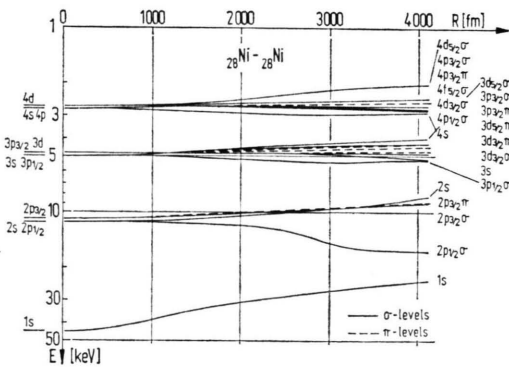

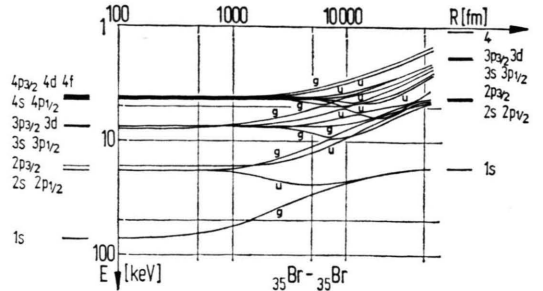Fig. 11. The asymptotic united atom region for the Ni+Ni system.

Fig. 12. The 16 lowest σ-levels of the Br+Br ($Z_1=Z_2=35$) molecular system in double-logarithmic scale. States of opposite parity are allowed to cross. The avoided crossing between the 2sσ and 3d$_{3/2}$σ states is magnified in Figure 3. Observe the 500 fm runway for 1sσ level.
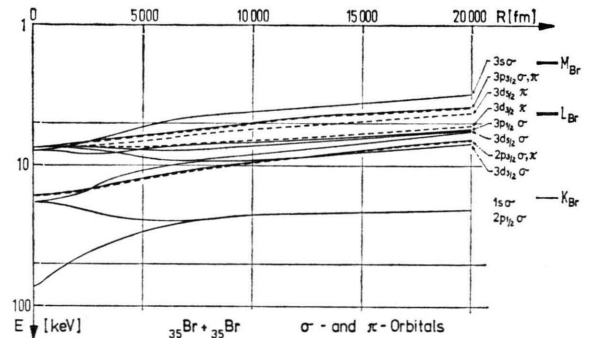

Fig. 13. The lowest 9 σ-states (solid lines) and four π-states of the Br+Br quasimolecule. The separation between the corresponding σ- and π-states is very small for the p-states, but larger for the d-states. The distance scale is linear.
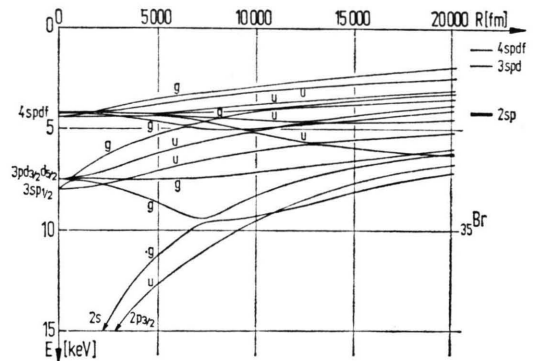

Fig. 14. The rearrangement region of the Br+Br system. The scale is linear and only the higher σ-orbitals are shown. Prominent features are the strongly promoted 3d$_{3/2}$σ and 4f$_{5/2}$σ molecular states.

stay almost constant. From this region one would expect to see the bulk of higher state MO-radiation ($R \leqq 10^4$ fm). The situation is a little different for the lowest molecular states. The 1sσ level reaches its united atom limit only at ca. $R = 500$ fm, if an unremovable 3 keV uncertainty due to experiment is attributed to the level. In a Ni−Ni collision this would mean that the united atom (Ba in this case) limit can be realized for a time of approx. 3×10^{-20} sec. A rough estimate indicates that this time should scale as $Z^{-1.5}$. This part of the level diagram is shown in greater detail in Figure 11.

All these comments hold with only slight quantitative adjustment for the energies and separations in the Br + Br system (Figures 12 − 14). One major

difference between these diagrams and the corresponding nonrelativistic ones is the fine-structure splitting between the 2p$_{1/2}$σ and 2p$_{3/2}$σ, π states in the united atom limit (see also Sect. XII). This

Table 2. The 1sσ wave function of the Br+Br quasimolecule at 8 internuclear separations from 200 to 10000 fm. Only the large ($s=1,2$) components of the expansion are given. Observe how the $l=2,4$ components increase as the separation R grows.

n	l	s	R= 200	500	1000	2000	3500	5000	7000	10000 (fm)
0	0	1	.08636	.17958	.26899	.35673	.38923	.39237	.35003	.37902
1			.00151	.00660	.01337	.02161	.02597	.02120	.02106	−.01997
2			.00036	.00121	.00269	.00292	.00536	.00643	.00567	−.00786
3			.00010	.00033	.00064	.00108	.00188	.00261	.00327	−.00378
4			.00003	.00011	.00021	.00035	.00061	.00097	.00141	−.00156
0	2	1	.01663	.04029	.07148	.10325	.17445	.21139	.25252	.28725
1			.00233	.00852	.01657	.02800	.03749	.04096	.07768	−.19901
2			.00057	.00222	.00447	.00701	.01444	.02382	.04971	−.08167
3			.00018	.00071	.00146	.00315	.00647	.00961	.01829	−.02188
4			.00007	.00024	.00054	.00116	.00247	.00447	.00745	−.00780
0	4	1	−.00959	−.02660	−.09422	−.20256	−.33912	−.43724	−.55694	−.18672
1			.00224	.00795	.01425	.02899	.05253	.08751	.20825	−.46428
2			.00046	.00187	.00380	.00842	.02441	.05464	.15504	−.27425
3			.00013	.00054	.00113	.00337	.00903	.01341	.02623	−.02879
4			.00004	.00018	.00038	.00111	.00306	.00593	.00827	−.00810
0	2	2	−.00050	−.00260	−.00794	−.02143	−.05131	−.08125	−.13991	−.00885
1			−.00002	−.00015	−.00067	−.00289	−.00680	−.00862	−.01455	−.01584
2			—	−.00002	−.00009	−.00028	−.00119	−.00266	−.00510	−.00752
3			—	—	−.00002	−.00008	−.00033	−.00062	−.00107	−.00168
4			—	—	—	−.00002	−.00008	−.00019	−.00028	−.00045
0	4	2	−.00041	−.00269	−.01237	−.03928	−.08859	−.13410	−.22028	.05790
1			−.00001	−.00008	−.00058	−.00287	−.00736	−.01113	−.02120	−.05960
2			—	−.00001	−.00006	−.00024	−.00103	−.00338	−.00891	−.02523
3			—	—	−.00001	−.00006	−.00025	−.00038	−.00060	−.00186
4			—	—	—	−.00001	−.00005	−.00011	−.00012	−.00031
Energy (keV)			−71.2	−65.4	−57.7	−46.0	−36.0	−29.5	−24.5	−18.2

Table 3. $2p_{3/2}\sigma$ molecular wave function in Br+Br is shown for internuclear separations R ranging from 200 to 10000 fm. For small R the (0,1,1) component is dominating, for large R the (0,1,2) component. This illustrate the angular momentum recoupling at $R \sim 500$ fm.

n	l	s	R= 200	500	1000	2000	3500	5000	7000	10000 (fm)
0	1	1	−.02403	−.06577	−.07278	−.03640	−.01630	−.00753	−.00578	−.00138
1			.00037	.01045	−.01221	−.05485	−.08827	−.12854	−.14310	−.14035
2			−.00093	−.00192	−.00371	−.00432	−.00989	−.02377	−.02197	−.01805
3			−.00028	−.00059	−.00120	−.00200	−.00417	−.00785	−.00926	−.00828
4			−.00009	−.00020	−.00043	−.00071	−.00146	−.00325	−.00312	−.00299
0	3	1	−.00859	−.01767	−.02658	−.02908	−.03243	−.05699	−.07117	−.09249
1			−.00277	−.00722	−.01289	−.01670	−.02579	−.04209	−.04739	−.05213
2			−.00082	−.00225	−.00459	−.00561	−.00895	−.01746	−.01616	−.01698
3			−.00026	−.00077	−.00161	−.00247	−.00402	−.00739	−.00879	−.00987
4			−.00010	−.00028	−.00061	−.00090	−.00154	−.00346	−.00357	−.00427
0	1	2	−.00387	−.02246	−.07245	−.17868	−.25729	−.38898	−.54523	−.79096
1			.00053	.00281	.00940	.02964	.03975	.06095	.09264	.13461
2			.00003	.00015	.00048	.00092	.00233	.00854	.01289	.01946
3			—	.00002	.00008	.00024	.00060	.00164	.00341	.00488
4			—	.00001	.00002	.00005	.00014	.00044	.00072	.00106
0	3	2	.00021	.00097	.00232	.00285	.00029	−.00225	−.01881	−.07381
1			.00003	.00016	.00056	.00161	.00325	.00578	.00884	.01616
2			—	.00003	.00009	.00020	.00059	.00189	.00252	.00386
3			—	.00001	.00002	.00006	.00018	.00049	.00092	.00156
4			—	—	.00001	.00001	.00002	.00005	.00016	.00024	.00036
Energy (keV)			−16.5	−16.5	−16.4	−15.6	−14.0	−12.4	−11.0	−9.5

feature becomes increasingly more important when the combined charge $Z_1 + Z_2$ of the system grows and can easily cause major deviations from a scaling law given by Briggs and Macek [55]. K-vacancy production cross sections could be influenced tremendously.

For this system (Br + Br) we also show the $1s\sigma$ and $2p_{3/2}\sigma$ wave functions for various distances (Tables 2 and 3). As remarked in Sect. IX, the wave functions were calculated in a basis of 100 states. The $s = 3,4$ components are small since the system is not extremely relativistic, also all components with wrong parity vanish identically. The values listed show how for $R \to \infty$ more and more components $P_l^m(\eta)$ are required to describe the wave function, whereas the convergence in $L_n^m(x)$ remains fast. One should observe that the basis functions are not orthonormal. Table 3 also illustrates the change from a $j = 3/2$ state at 200 fm to an almost pure $l = 1$ state at 200 fm, which was predicted for the $2p_{3/2}\sigma$ level in Section XII. After these symmetric systems we consider a slightly asymmetric combination, Br + Zr (i. e. $Z_1 = 35$, $Z_2 = 40$). As discussed in Sect. X, states do not have good parity and all crossings between σ states are avoided. Since the parity non-conserving part of the potential is weak $[\Delta Z/(Z_1 + Z_2) \ll 1]$, in an actual time-dependent process the diabetic states will prevail. Interesting features of the diagram (Figs. 15, 16) are the "diabatic" $4f_{5/2}\sigma$ level between 8000 and 20000 fm and the rather close approach between the $1s\sigma$ and $2p_{1/2}\sigma$ MO-states at ca. 10000 fm. The latter one has been extensively discussed in Sect. XI b and Figure 5.

Fig. 16. The rearrangement region in the Br + Zr system in linear scale. No crossing between the adiabatic states are allowed. Observe the strongly promoted $4f_{5/2}\sigma$ states.
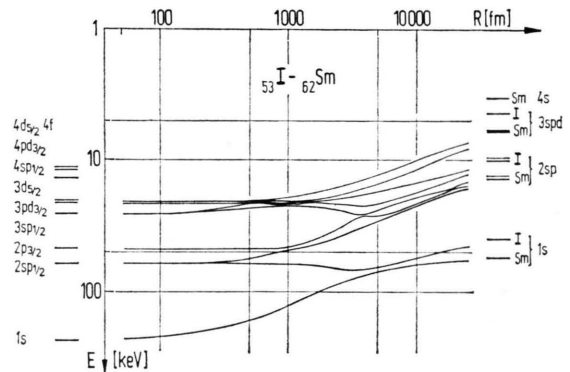
Fig. 17. The 9 lowest σ-states of the molecular system I + Sm ($Z_1 = 53$, $Z_2 = 62$). This system might be of interest because the Sm-nucleus has a low-lying 2^+ state so that mixing between nuclear and electronic transitions may occur.
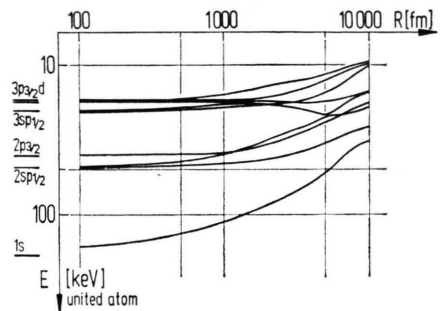

Fig. 18. The I + I system ($Z_1 = Z_2 = 53$) in double-logarithmic scale. The 9 lowest molecular σ-levels are shown.

Another system of very similar structure is the I (53) + Sm (62) shown in Figure 17. Since the relative asymmetry is rather close to Br + Zr we refrain from a detailed explanation of the figure.

The second di-halide system we shall discuss is the I + I quasimolecule (Figs. 18 and 19). There
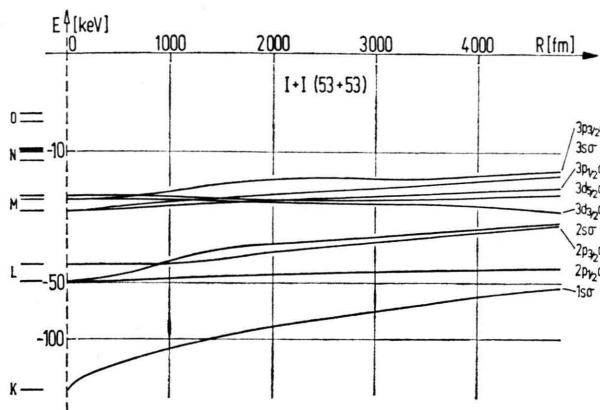

Fig. 15. The 13 lowest σ-states in the Br + Zr ($Z_1 = 35$, $Z_2 = 40$) quasimolecule. All crossings are avoided in this asymmetric system. The approach between the $1s\sigma$ and $2p_{1/2}\sigma$ states is shown in detail in Figure 5. The scale is double logarithmic.

Fig. 19. The I+I quasimolecular states in a linear distance scale for small internuclear separations.
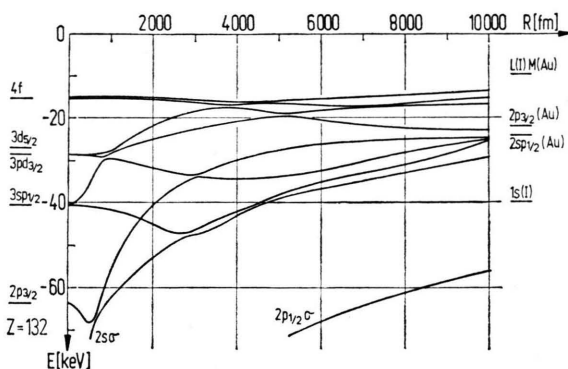

Fig. 21. The I+Au rearrangement region. Only the higher states are shown. The deep dip in the $2p_{3/2}\sigma$ level is peculiar to a highly relativistic asymmetric system where Sect. XII does not apply because of the large $2p_{3/2}-2p_{1/2}$ splitting.

are no principle differences to the Br + Br system shown earlier in this section, but relativistic effects on binding begin to play a more important role. The $2p_{1/2}$ level of the compound atom $Z = 106$ (in the one-electron approximation!) is by about 10 keV lower than the 1s level in iodine. Therefore, the dip in the $2p_{1/2}\sigma$ molecular state is much less striking in truly non-relativistic systems.

A third molecular system having iodine as the one partner is of particular experimental interest [11, 56]: I(53) + Au(79). The united atom $Z = 132$ is the first superheavy quasi-atom which seems to be so far produced (except for observations of Kaun et al. for $Z = 57$ collisions [14a]). As it is still below the critical charge for point nuclei the united atom limit exists for all MO level if point nuclear charges are taken. The level diagram is presented

in Figs. 20 and 21. One of the most interesting features is the very strong spin-orbit splitting between the $2p_{1/2}$ and $2p_{3/2}$ states in the $Z = 132$ united atom. Consequently, the $2p_{3/2}\sigma$ molecular level is initially lowered dramatically, until the angular momentum recoupling process of Sect. XII causes it to rise again at approximately $R = 500$ fm. Only in this case of a strongly asymmetric system the molecular dipole moment plays the important role. The strongly promoted $3d_{3/2}\sigma$ and $4f_{5/2}\sigma$ levels behave as they do in lighter systems.

Figure 22 shows the Ho + Ho system ($Z_1 = Z_2 = 67$) which has a united atom just below the critical limit of point charges. It is seen that the $j = 1/2$ levels increase steeply in binding energy as $R \to \infty$, but they still attain a limit for $R = 0$.
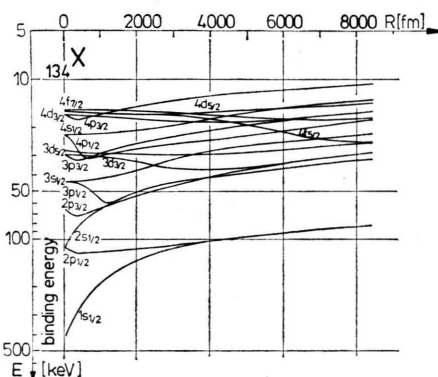

Fig. 20. The I+Au ($Z_1 = 53$, $Z_2 = 79$) quasimolecule in double-logarithmic presentation. Eleven σ-states are shown. The 4f−3d transitions have been of particular interest. This is the first superheavy system investigate in experiment. The $2p_{1/2}-2p_{3/2}$ splitting is 30 keV and the 1sσ states eventually gains 300 keV in binding energy.

Fig. 22. The 16 lowest σ-states of the Ho+Ho molecule ($Z_1 = Z_2 = 67$) for point nuclei. The $j = 1/2$ states just reach finite limits in the united atom limit. The diabatic representation is used.

We turn to an extremely asymmetric system, which also has been of considerable experimental interest [13, 57]: Cl + Pb ($Z_1 = 17$, $Z_2 = 82$). The level diagram is shown in Figure 23. Only the four lowest molecular states are given, since in an actual collision the higher states will not be adiabatic. This is the limiting case in which the description by molecular states goes over into the perturbation of atomic states by a small incident charge. The chlorine levels do not mix — up to the M-shell — with the lead levels to cause promotion or demotion. Thus one would not expect to see prominent molecular features in an experiment but rather explain the

results by polarization of the Pb target by the small Cl projectile.

Finally, we present the U + U system (Figs. 24 — 26) which is completely dominated by relativistic effects. The most important one — conceptually — is that the $1s\sigma$ molecular level joins the negative energy Dirac continuum, a fact already discussed in Section XIII. But, apart from this: the spatial extension of the two nuclei becomes crucial to the limit one obtains for zero internuclear separation (Section VIII). The $np_{1/2}$ states in the united atom limit are considerably more strongly bound than the corresponding $ns_{1/2}$ states. This makes more than $550\,\text{keV}$ for the $2p_{1/2}$ and $2s_{1/2}$ levels.

Fig. 23. The Cl + Pb system ($Z_1 = 17$, $Z_2 = 82$) in a linear scale. Only the four lowest σ-states are shown. The system is extremely asymmetric, so that up to the M-shell the molecular states are formed without the participation of the chlorine atomic levels. This puts the system at the fringe of the molecular model.
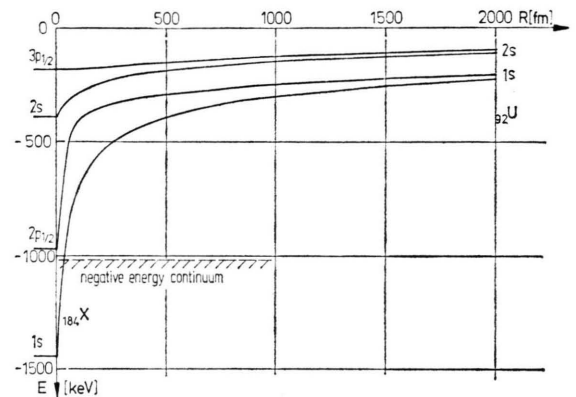

Fig. 25. The four highly relativistic molecular states in the U + U diagram in a linear scale. The strong increase in binding takes place below $R = 150$ fm. See also Figure 8.
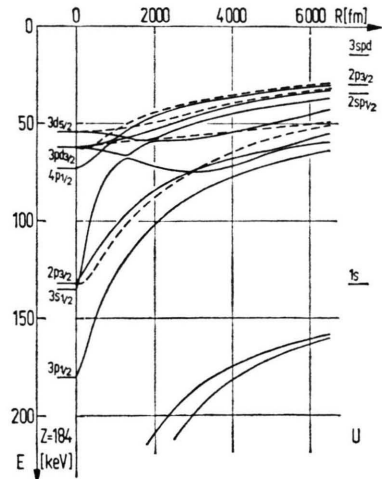

Fig. 24. The 10 lowest σ-levels and four π-levels of the supercritical U + U ($Z_1 = Z_2 = 92$) quasimolecule. The states are calculated with extended nuclear charge distribution; the spectrum is cut off at the Coulomb barrier ($R = 15$ fm). Note that the $1s\sigma$ state reaches the lower Dirac continuum around $R = 35$ fm.

Fig. 26. The rearrangement region in the U + U quasimolecule. σ-states (solid lines) and π-states (broken lines) are given. Due to relativistic effects, the σ- and π-states are no more almost degenerate. Linear scale.

Finally the "fine-structure" splitting between $2p_{1/2}$ and $2p_{3/2}$ states is tremendous: 800 keV in the united atom ($Z = 184$) limit.

After the discussion of other diagrams, Figs. 24 and 25 are rather self-explanatory. The $1s\sigma$ MO state turns out to be almost a straight line in the double-logarithmic Fig. 24, i.e. it is of the form
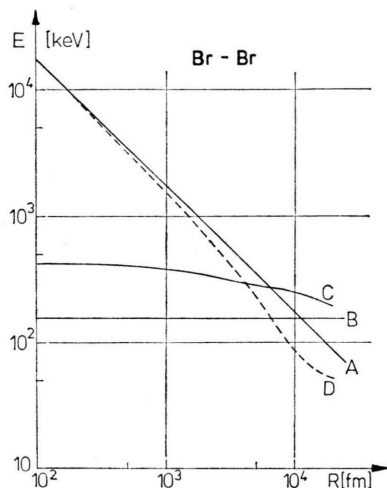

Fig. 27. The molecular potential in the Br+Br system. All states shown in Fig. 13 are included. (A) Coulomb repulsion between the nuclei; (B) electronic binding energy in the separate systems; (C) electronic binding energy in the quasimolecule and (D) total molecular potential. At large separations electron shielding becomes important, causing strong deviations from this figure, which was obtained by summing one-electron energies.
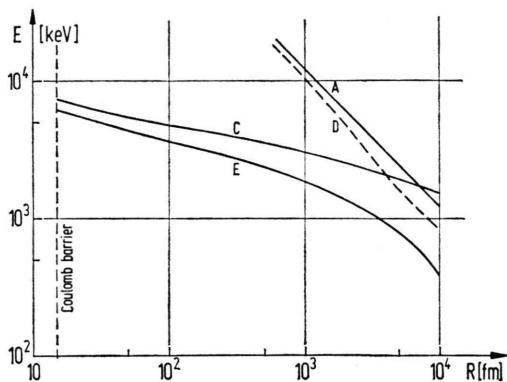

Fig. 28. The molecular potential in the U+U system. All states from Fig. 24 are taken into account. (A) Coulomb repulsion between the nuclei; (C) electronic binding in the molecule; (D) the total molecular potential and (E) the gain in electronic binding energy in the molecule. This gain amounts to more than 6 MeV at the Coulomb barrier, causing deviations up to 3 percent in differential scattering cross sections.

$E \sim r^{-\alpha}$. This makes it possible to extract its actual energy out of X-ray anisotropy measurements [58]. To Fig. 26 it is worthwhile to note that (due to the strong shift of the $np_{1/2}$ united atom states) the scheme deviates from lighter diagrams in the course of the $np_{1/2}\sigma$ and $np_{3/2}\sigma$ molecular levels. So e. g. the $3p_{3/2}\pi$ state becomes the spin-flipped counterpart of the $4p_{1/2}\sigma$ MO level.

With this remark we conclude the presentation of various molecular level schemes and finally give the full molecular potentials for the Br+Br system (Fig. 27) and the U+U system (Figure 28). Except for very large distances, the deviations of the total molecular potential curve from the $1/r$-Coulomb repulsion between the two nuclei are seen to be smooth. However, for U+U the potential contribution from electronic molecular binding attains more than 6 MeV at the Coulomb barrier. The deviations from Rutherford scattering due to the electronic contribution have been calculated in the classical approximation by Rafelsky [59b] and Schäfer and by Soff [59a]. The U+U potential (E), which can be parametrized by

$$V_{el} \sim V_0 \left(\frac{R}{R_0} \right)^{-0.27} e^{-R/R_1} \qquad (14.1)$$

with $V_0 = 3640$ keV, $R_0 = 100$ fm and $R_1 = 10^4$ fm, leads to 3% deviation in forward collisions down to 1% in backward scattering. This has to be compared with at most 1% deviation from vacuum polarization effects between the two nuclei [59b], indicating that the molecular potential might be deducible from differential scattering cross section measurements.

It should be stressed that the potential curves were obtained from the one-electron energies calculated earlier. One expects qualitative deviations in the asymptotic region of very large separations if screening is taken into account. For separations below ca. 3000 fm the corrections can be estimated to be $10 - 20\%$ of the electronic binding contribution.

Summary and Outlook

In this article we have outlined the mathematical and physical problems connected with the Two-Centre Dirac Equation. Its solutions were presented for various symmetric and asymmetric systems. They have to be extended in future works to include electronic shielding and are absolutely essential for any

calculation of intermediate molecular phenomena, occurring in atom-atom collisions. The most important of these are the molecular X-rays and the positron-decay of the neutral vacuum in overcritical fields. At present, only the molecular X-rays in heavy ion collisions are accessible to experiments, and they themselves are indeed interesting enough to furnish a rich field of research. Experimentally [11, 15] directional anisotropy of molecular radiation has been discovered which seems to peak near the classical endpoint of the non-characteristic spectrum. Theoretically [34, 60] it was shown that alignment of the various molecular orbitals can lead to such an effect. Eventually, it might prove useful in the spectroscopy of superheavy intermediate molecular orbitals. Many more of these effects will be discovered in the future; most of them will be connected with interference phenomena occurring in the collisions of heavy ions. Particularly coincidence experiments between scattered ion and X-ray will furnish insight into the mechanisms and usefulness of the various approximations.

Appendix A

Evaluation of the Spinor Connections Γ_k

Using the metric tensor given by (3.4) one easily confirms that the only nonvanishing Christoffel symbols are

$$\left\{ \begin{matrix} 1 \\ 24 \end{matrix} \right\} = -\frac{\omega}{c}\,; \quad \left\{ \begin{matrix} 1 \\ 44 \end{matrix} \right\} = -\frac{\omega^2}{c^2}\,x\,;$$

$$\left\{ \begin{matrix} 2 \\ 14 \end{matrix} \right\} = \frac{\omega}{c}\,; \quad \left\{ \begin{matrix} 2 \\ 44 \end{matrix} \right\} = -\frac{\omega^2}{c^2}\,y\,. \quad (A.1)$$

Inserting these one finds that

$$\hat{\gamma}_{i|k} - \left\{ \begin{matrix} l \\ i\,k \end{matrix} \right\} \hat{\gamma}_l = \begin{pmatrix} 0 & \boldsymbol{s} \\ 0 & F \end{pmatrix} \quad (A.2)$$

with

$$F = \frac{\omega^2}{c^2}\,(x\,\gamma_1 + y\,\gamma_2) + \frac{\dot{\omega}}{c^2}\,(x\,\gamma_2 - y\,\gamma_1) \quad (A.3)$$

$$= \left(\frac{\omega}{c} \times \boldsymbol{r} \right) \cdot \left(\frac{\omega}{c} \times \boldsymbol{\gamma} \right) + \left(\frac{\dot{\omega}}{c^2} \times \boldsymbol{r} \right) \cdot \boldsymbol{\gamma}$$

and

$$\boldsymbol{s} = \left\{ -\frac{\omega}{c}\,\gamma_2, \ \frac{\omega}{c}\,\gamma_1, 0 \right\} = \left(\frac{\omega}{c} \times \boldsymbol{\gamma} \right). \quad (A.4)$$

Then the first term in eq. (3.2) becomes

$$\hat{\gamma}^k \hat{\gamma}^i \left(\hat{\gamma}_{i|k} - \left\{ \begin{matrix} l \\ i\,k \end{matrix} \right\} \hat{\gamma}_l \right) = -\gamma_4 \left(\boldsymbol{\gamma} + \left(\frac{\omega}{c} \times \boldsymbol{r} \right) \gamma_4 \right) \cdot \boldsymbol{s}$$

$$+ \gamma_4\,\gamma_4\,F = \gamma_4\,\boldsymbol{\gamma} \cdot \boldsymbol{s} - \left(\frac{\dot{\omega}}{c^2} \times \boldsymbol{r} \right) \cdot \boldsymbol{\gamma}$$

$$= \gamma_4\,\frac{\omega}{c} \cdot (\boldsymbol{\gamma} \times \boldsymbol{\gamma}) - \left(\frac{\dot{\omega}}{c^2} \times \boldsymbol{r} \right) \cdot \boldsymbol{\gamma}\,. \quad (A.5)$$

To evaluate the second term, the trace part of (3.3), we first note that

$$\hat{\gamma}^i \hat{\gamma}_{i|k} = \gamma_4 \left\{ \frac{\omega}{c} \times \boldsymbol{\gamma}, \ -\left(\frac{\dot{\omega}}{c^2} \times \boldsymbol{r} \right) \cdot \boldsymbol{\gamma} \right\} \quad (A.6)$$

and that

$$\hat{\gamma} = \gamma + \sum_{\text{some permutations}} \left[(\pm)\,\frac{\omega}{c}\,y\,\gamma_2\,\gamma_3 (\pm)\,\frac{\omega}{c}\,x\,\gamma_1\,\gamma_3 \right] \quad (A.7)$$

Now it is known that

$$\text{trace}\,(\gamma) = \text{trace}\,(\gamma_2\,\gamma_3) = \text{trace}\,(\gamma_1\,\gamma_3) = 0\,. \quad (A.8)$$

Hence that second part vanishes and we have

$$\hat{\gamma}^k\,\Gamma_k = \frac{1}{4}\,\gamma_4\,\frac{\omega}{c} \cdot (\boldsymbol{\gamma} \times \boldsymbol{\gamma}) - \frac{1}{4} \left(\frac{\dot{\omega}}{c^2} \times \boldsymbol{r} \right) \cdot \boldsymbol{\gamma}\,. \quad (A.9)$$

Appendix B

Recursive Evaluation of the Matrix Elements

A glance at the definition of the diagonal matrix Φ_m (6.7) shows that $\Phi_m^+\,\Phi_m$ is independent of the variable φ. Therefore the integration over $d\varphi$ in all matrix elements (7.14) and (7.15) yields 2π, and, in order to get rid of useless constants, we divide the matrix elements — or equivalently, the Hamiltonian — by $2\pi R^2 a$. Observe that a is the same for all wave functions! This is allowed since, of course, the Hamiltonian commutes with a constant.

After that, the integration in the matrix elements covers the range $(\xi = a\,x + 1)$:

$$R \int_0^\infty \mathrm{d}x \int_{-1}^{+1} \mathrm{d}\eta \, (\xi^2 - \eta^2) \tag{B.1}$$

Application of the following recursive relations [63-66] among the L_n^α and P_l^α permits to carry out all matrix elements without performing explicit integrations.

a) For the $L_n^\alpha(x)$:

$$L_n^{\alpha-1}(x) = L_n^\alpha(x) - L_{n-1}^\alpha(x) , \tag{B.2}$$

$$L_n^{\alpha+1}(x) = \sum_{\nu=0}^n L_\nu^\alpha(x) , \tag{B.3}$$

$$L_n^{\alpha+\beta}(x) = \sum_{\nu=0}^n \binom{\alpha+\beta-\nu-1}{\beta-1} L_\nu^\alpha(x) , \tag{B.4}$$

$$x\,L_n^\alpha(x) = (2\,n+\alpha+1)\,L_n^\alpha(x) \\ - (n+\alpha)\,L_{n-1}^\alpha(x) - (n+1)\,L_{n+1}^\alpha(x) , \tag{B.5}$$

$$x\,L_n^{\alpha+1}(x) = (n+\alpha+1)\,L_n^\alpha(x) - (n+1)\,L_{n+1}^\alpha(x) , \tag{B.6}$$

$$\frac{\mathrm{d}}{\mathrm{d}x}\,L_n^\alpha(x) = -L_{n-1}^{\alpha+1}(x) , \tag{B.7}$$

$$x\,\frac{\mathrm{d}}{\mathrm{d}x}\,L_n^\alpha(x) = n\,L_n^\alpha(x) - (n+\alpha)\,L_{n-1}^\alpha(x) . \tag{B.8}$$

b) For the $P_l^\alpha(\eta)$:

$$(2\,l+1)\,\eta\,P_l^\alpha(\eta) = (l-\alpha+1)P_{l+1}^\alpha(\eta) + (l+\alpha)P_{l-1}^\alpha(\eta) , \tag{B.9}$$

$$(2\,l+1)\sqrt{1-\eta^2}\,P_l^{\alpha-1}(\eta) = P_{l-1}^\alpha(\eta) - P_{l+1}^\alpha(\eta) , \tag{B.10}$$

$$\sqrt{1-\eta^2}\,P_l^{\alpha+1}(\eta) = (l-\alpha)\eta\,P_l^\alpha(\eta) - (l+\alpha)P_{l-1}^\alpha(\eta) , \tag{B.11}$$

$$\sqrt{1-\eta^2}\,\frac{\mathrm{d}}{\mathrm{d}\eta}\,P_l^\alpha(\eta) = -P_l^{\alpha+1}(\eta) - \frac{\alpha\,\eta}{\sqrt{1-\eta^2}}\,P_l^\alpha(\eta) , \tag{B.12}$$

$$\sqrt{1-\eta^2}\,\frac{\mathrm{d}}{\mathrm{d}\eta}\,P_l^\alpha(\eta) = (l+\alpha)\,(l-\alpha+1)P_l^{\alpha-1}(\eta) + \frac{\alpha\,\eta}{\sqrt{1-\eta^2}}\,P_l^\alpha(\eta) , \tag{B.13}$$

$$(1-\eta^2)\,\frac{\mathrm{d}}{\mathrm{d}\eta}\,P_l^\alpha(\eta) = (l+\alpha)P_{l-1}^\alpha(\eta) - l\,\eta\,P_l^\alpha(\eta) . \tag{B.14}$$

All integrals can be separated into integrals over $\mathrm{d}x$ and those over $\mathrm{d}\eta$. We give the recursive evaluation of all integrals occurring as parts of the matrix element (7.14) and (7.15).

c) For the $\mathrm{d}x$ integrals we introduce the abbreviation

$$\langle n'\,\alpha'\,|\,\hat{A}\,|\,n\,\alpha\rangle = \int_0^\infty e^{-x/2}\,L_{n'}^{\alpha'}(x)\,\hat{A}\,e^{-x/2}\,L_n^\alpha(x)\,\mathrm{d}x \tag{B.15}$$

where $\hat{A}$ is any operator on $\{x\,|\,0 \leq x\}$. The fundamental integral is the orthogonality relation

$$L_0(n',n,\alpha) \equiv \langle n'\,\alpha\,|\,x^\alpha\,|\,n\,\alpha\rangle = \frac{\Gamma(n+\alpha+1)}{\Gamma(n+1)}\,\delta_{n'n} . \tag{B.16}$$

To this relation all following integrals are reduced step by step:

$$L_\beta(n',n,\alpha) = \langle n'\,\alpha\,|\,x^{\alpha+\beta}\,|\,n\,\alpha\rangle \\ = (2\,n+\alpha+1)\,(L_{\beta-1}(n',n,\alpha) - (n+\alpha)\,L_{\beta-1}(n',n-1,\alpha) - (n+1)\,L_{\beta-1}(n',n+1,\alpha) \tag{B.17}$$

for $\beta = 1, 2, 3, \ldots$;

$$L_{0\mathrm{R}}(n',n,\alpha) = \langle n'\,\alpha\,|\,x^\alpha\,|\,n\,\alpha+1\rangle = \sum_{\nu=0}^n L_0(n',\nu,\alpha) , \tag{B.18}$$

$$L_{\beta\mathrm{R}}(n',n,\alpha) = \langle n'\,\alpha\,|\,x^{\alpha+\beta}\,|\,n\,\alpha+1\rangle = L_{\beta-1}(n',n,\alpha+1) - L_{\beta-1}(n'-1,n,\alpha+1) \tag{B.19}$$

for $\beta = 1, 2, 3, \ldots$;

$$L_{\beta\mathrm{L}}(n',n,\alpha) = \langle n'\,\alpha+1\,|\,x^{\alpha+\beta}\,|\,n\,\alpha\rangle = L_{\beta\mathrm{R}}(n,n',\alpha) \tag{B.20}$$

for all $\beta = 0, 1, 2, \ldots$.

Furthermore, one has the following integrals with differential operators:

$$L_{\beta D}(n', n, a) = \langle n' a \,|\, x^{a+\beta} \frac{\mathrm{d}}{\mathrm{d}x} \,|\, n a \rangle = n L_{\beta-1}(n', n, a) - (n+a) L_{\beta-1}(n', n-1, a) - \tfrac{1}{2} L_\beta(n', n, a) \quad \text{(B.21)}$$

for $\beta = 1, 2, 3, \ldots$;

$$L_{1DR}(n', n, a) = \langle n' a \,|\, x^{a+1} \frac{d}{\mathrm{d}x} \,|\, n a+1 \rangle = \tfrac{1}{2}(n-a-1) L_0(n', n, a)$$
$$+ \tfrac{1}{2}(n+1) L_0(n', n+1, a) - (a+1) L_{0R}(n', n-1, a), \quad \text{(B.22)}$$

$$L_{\beta DR}(n', n, a) = \langle n' a \,|\, x^{a+\beta} \frac{d}{\mathrm{d}x} \,|\, n a+1 \rangle = L_{(\beta-1)D}(n', n, a+1) - L_{(\beta-1)D}(n'-1, n, a+1) \quad \text{(B.23)}$$

for $\beta = 2, 3, 4, \ldots$; and finally

$$L_{\beta DL}(n', n, a) = \langle n' a+1 \,|\, x^{a+\beta} \frac{\mathrm{d}}{\mathrm{d}x} \,|\, n a \rangle = -\tfrac{1}{2} L_{\beta L}(n', n, a) - L_{\beta-1}(n', n-1, a+1) \quad \text{(B.24)}$$

for $\beta = 1, 2, 3, \ldots$.

d) for the integrals over $\mathrm{d}\eta$ involving the Legendre polynomials we introduce an analogous abbreviation

$$\langle l' a' \,|\, \hat{A} \,|\, l a \rangle = \int_{-1}^{+1} P_{l'}^{a'}(\eta) \,\hat{A}\, P_l^{a}(\eta) \, \mathrm{d}\eta . \quad \text{(B.25)}$$

Here the fundamental orthogonality relation is

$$P_0(l', l, a) = \langle l' a \,|\, l a \rangle = \frac{2 \, \Gamma(l+a+1)}{(2 l+1) \, \Gamma(l-a+1)} \, \delta_{l'l} . \quad \text{(B.26)}$$

The reducible integrals are:

$$P_\beta(l', l, a) = \langle l' a \,|\, \eta^\beta \,|\, l a \rangle$$
$$= \frac{l-a+1}{2 l+1} P_{\beta-1}(l', l+1, a) + \frac{l+a}{2 l+1} P_{\beta-1}(l', l-1, a) \quad \text{(B.27)}$$

for all $\beta = 1, 2, 3, \ldots$;

$$P_{SQR}(l', l, a) = \langle l' a \,|\, \sqrt{1-\eta^2} \,|\, l a+1 \rangle = (l-a) P_1(l', l, a) - (l+a) P_0(l', l-1, a) ; \quad \text{(B.28)}$$

$$P_{SQL}(l', l, a) = \langle l' a+1 \,|\, \sqrt{1-\eta^2} \,|\, l a \rangle = P_{SQR}(l, l', a) \quad \text{(B.29)}$$

and three integrals involving differential operators:

$$P_D(l', l, a) = \langle l' a \,|\, (1-\eta^2) \frac{\mathrm{d}}{\mathrm{d}\eta} \,|\, l a \rangle = (l+a) P_0(l', l-1, a) - l P_1(l', l, a) ; \quad \text{(B.30)}$$

$$P_+(l', l, a) = \langle l' a+1 \,|\, -\sqrt{1-\eta^2} \, \eta \frac{\mathrm{d}}{\mathrm{d}\eta} - \frac{a \eta^2}{\sqrt{1-\eta^2}} \,|\, l a \rangle = P_1(l', l, a+1) ; \quad \text{(B.31)}$$

$$P_-(l', l, a) = \langle l' a \,|\, -\sqrt{1-\eta^2} \, \eta \frac{\mathrm{d}}{\mathrm{d}\eta} + \frac{(a+1)\eta^2}{\sqrt{1-\eta^2}} \,|\, l a+1 \rangle = -(l-a)(l+a+1) P_1(l', l, a) . \quad \text{(B.32)}$$

Since the denominator $(\xi^2 - \eta^2)$ in the constituents of the operator π_m (6.8) and the potential (5.16) is cancelled by the factor $(\xi^2 - \eta^2)$ in the volume element (5.17), all matrix elements of the Hamiltonian (7.14) and (7.15) are linear combinations of the integrals given above in (B.16) to (B.32). It should be mentioned that in all formulae of this Appendix the positive value $|m|$ of the angular momentum projection $m = \langle J_z \rangle$ has to be taken ($a \geq 0$). For problems with negative values of m we refer to the end of Chapter VI.

Appendix C

A Quadrature Formula for Exponential Integrals

If one takes different scaling parameters a_{nl} for the different basis functions (7.1), the variable x is differently defined in each case:

$$x_{nl} = (\xi - 1)/a_{nl} \qquad (C.1)$$

No orthogonality relation exists for integrals with Laguerre polynomials depending on different variables. There are, however, quadrature formulas of the type

$$\int_0^\infty x^a e^{-x} f(x) \, dx = \sum_{i=1}^n \omega_i f(x_i) + R_n \qquad (C.2)$$

which help to solve the integrals even in this case [67, 68]. The x_i are the n zeros of the associated Laguerre polynomial $L_n^a(x)$ and the weights ω_i are defined by

$$\omega_i = \frac{\Gamma(n+1)\,\Gamma(n+a+1)}{\dfrac{d}{dx}\,[L_n^a(x)]\big|_{x=x_i} L_{n-1}^\alpha(x_i)} . \qquad (C.3)$$

The point is, that the remainder R_n depends only on the $(2n)$-th derivative of the function $f(x)$ in (C.2):

$$R_n \sim f^{(2n)}(z) \quad (0 \leqq z < \infty) . \qquad (C.4)$$

Whenever $f(x)$ is a polynomial of degree N, it is sufficient to choose $2n > N$ in order to insure $f^{(2n)}(x) \equiv 0$ everywhere.

For all our matrix elements this condition is satisfied: $f(x)$ is a product of two Laguerre polynomials, a power of x and — possibly — the differential operator d/dx. With the help of the recurrence relations (B.7) and (B.8) the derivative can be replaced and one is left with

$$f(x) = L_{n'}^{\alpha'}(x)\, L_n^\alpha \left(\frac{a_{n'l'}}{a_{nl}}\, x \right) \sum_{i=0}^k c_i x^i . \qquad (C.5)$$

The $(n' + n + k + 1)$-th derivative of $f(x)$ vanishes identically and therefore $R_N = 0$ in (C.2), and the quadrature is exact with a finite number of points to be taken. Thus this is a finite algebraical procedure, too. It turns out to be better suited for computer programming than the recursive method sketched in Appendix B. Of course, now the Hamiltonian may be divided only by $2\pi R^2$. For the integrals over $d\eta$, however, it is convenient to use the recurrence relation given in Appendix B.

[1] U. Fano and W. Lichten, Phys. Rev. Lett. **14**, 627 [1965].

[2] M. Barat and W. Lichten, Phys. Rev. **A 6**, 211 [1972].

[3] F. T. Smith, Phys. Rev. **179**, 111 [1969]. This paper has been critically commented on by H. Gabriel and K. Taulbjerg, Phys. Rev. **A 10**, 741 [1974].

[4a] D. A. Bromley, Int. Conf. on Heavy Ions, ed. R. Bock and W. Hering, North Holland Publishing Company, Heidelberg 1969, p. 27.

[4b] W. Greiner, ibid. p. 748; P. Holzer, U. Mosel, and W. Greiner, Nucl. Phys. **A 138**, 241 [1969]; D. Scharnweber, U. Mosel, and W. Greiner, Phys. Lett. **24**, 601 [1970].

[5] W. Pieper and W. Greiner, Z. Physik **218**, 327 [1969]; W. Greiner, Panel Discussion, Proceedings Int. Conf. on Properties of Nuclear States, Montreal 1969, p. 605. The idea of intermediate electronic superheavy molecules has first been mentioned by the authors in GSI-seminars during 1969—1972, see e. g. the report by P. H. Mokler, GSI-Bericht 72-7; available from Gesellschaft für Schwerionenforschung, D-6100 Darmstadt. It has first been published in a journal by J. Rafelski, L. Fulcher, and W. Greiner, Phys. Rev. Lett. **27**, 958 [1971].

[6a] B. Müller, H. Peitz, J. Rafelski, and W. Greiner, Phys. Rev. Lett. **28**, 1235 [1972].

[6b] B. Müller, J. Rafelski, and W. Greiner, Z. Physik **257**, 62 [1972]; ibid. **257**, 183 [1972].

[7] J. Rafelski, B. Müller, and W. Greiner, Nucl. Phys. **B 68**, 585 [1974].

[8] H. Peitz, B. Müller, J. Rafelski, and W. Greiner, Lett. Nuovo Cim. **8**, 37 [1972].

[9] Ya. B. Zeldovich and V. S. Popov, Sov. Phys. Uspekhi **14**, 673 [1972].

[10] F. W. Saris, W. F. van der Weg, H. Tawara, and W. A. Laubert, Phys. Rev. Lett. **28**, 717 [1972]; J. Physics B, in press.

[11] P. H. Mokler, H. J. Stein, and P. Armbruster, Phys. Rev. Lett. **29**, 827 [1972]; G. Kraft, P. H. Mokler, and H. J. Stein, Phys. Rev. Lett. **33**, 475 [1974]; P. H. Mokker, G. Kraft, and H. J. Stein, Proceedings Int. Conf. on Reactions between Complex Nuclei, Nashville, Tenn., June 1974, Vol. 1,, p. 134, North Holland Publ. Comp., Amsterdam. — The I-Au system has also been extensively investigated with great accuracy by H. E. Gove et al. (University of Rochester, to be published), and by W. Wölfli and collaborators, ETH Zürich, private communication.

[12] a) J. R. MacDonald, M. D. Brown, and T. Chiao, Phys. Rev. Lett. **30**, 471 [1973]. — b) W. E. Meyerhof, T. K. Saylor, S. M. Lazarus, W. A. Little, and B. B. Triplett, Phys. Rev. Lett. **30**, 1279 [1973] and (together with R. Anholt), Phys. Rev. Lett. **32**, 502 [1974].

[13] D. Burch, W. B. Ingalls, H. Wieman, and R. Vandenbosch, University of Washington, Seattle, preprint and private communication (1973/74).

[14] a) P. Gippner, K.-H. Kaun, F. Stary, W. Schulze, and Yu. P. Tretyakov, Nucl. Phys. **A 230**, 509 [1974]; b) K. O. Groeneveld, B. Knaf, and G. Presser, Proc. Int. Conf. on Reactions between Complex Nuclei, Nashville, Tenn., June 1974, vol. 1, p. 133, North-Holland Publ. Comp., Amsterdam.

[15] C. K. Davis and J. S. Greenberg, Phys. Rev. Lett. **32**, 1215 [1974]; J. S. Greenberg, C. K. Davis, and P. Vincent, Phys. Rev. Lett. **33**, 473 [1974]; J. S. Greenberg, C. K. Davis, B. Müller, and W. Greiner, Proceedings of the Int. Conf. on Reactions between Complex Nuclei, Nashville, Tenn., June 1974.

[16] P. G. Reinhard, W. Greiner, and H. Arenhövel, Nucl. Phys. A **166**, 173 [1971].

[17] Estimates of vacuum polarization with limiting field electrodynamics have been given by G. Soff, J. Rafelski, and W. Greiner, Phys. Rev. A **7**, 903 [1973]. Rigorous calculations have been carried out by M. Gyulassy, Phys. Rev. Lett. **33**, 921 [1974] and by G. Rinker and L. Wilets, Phys. Rev. A **12**, 748 [1975].

[18] G. Soff, B. Müller, and J. Rafelski, Z. Naturforsch. **29 a**, 1267 [1974].

[19] K. Smith, H. Peitz, B. Müller, and W. Greiner, Phys. Rev. Lett. **32**, 554 [1974].

[20] W. Heitler and F. London, Z. Physik **44**, 455 [1927].

[21] E. Teller, Z. Physik **61**, 458 [1930].

[22] F. A. Hylleraas, Z. Physik **71**, 739 [1931].

[23] G. Jaffé, Z. Physik **87**, 535 [1934].

[24] K. Helfrich and H. Hartmann, Theor. Chim. Acta **3**, 21 [1965].

[25] K. Helfrich and H. Hartmann, Theor. Chim. Acta **10**, 406 [1968]; ibid. **16**, 263 [1970]; ibid. **21**, 44 [1971].

[26] F. Larkins, J. Phys. B **5**, 571 [1972].

[27] S. K. Luke et al., J. Chem. Phys. **50**, 1644 [1969].

[28] K. Smith, B. Müller, and W. Greiner, J. Phys. B **8**, 75 [1975].

[29] J. Eisenberg and W. Greiner, Nuclear Theory, Vol. 2, p. 214, North Holland Publishing Company, Amsterdam 1970.

[30] H. Tetrode, Z. Physik **50**, 336 [1928].

[31] V. A. Fock and D. Ivanenkov, Z. Physik **57**, 261 [1929].

[32] E. Schmutzer, Relativistische Physik, Teubner, Leipzig 1960. See also, the review article of W. L. Bade and H. Jehle, Rev. Mod. Phys. **25**, 714 [1953] and for a representation in Cartan frames the work of D. R. Brill and J. M. Cohen, J. Math. Phys. **7**, 238 [1966].

[33] B. Müller, K. Smith, and W. Greiner, Phys. Lett. **49 B**, 219 [1974].

[34] a) B. Müller and W. Greiner, Phys. Rev. Lett. **33**, 469 [1974].

[35] C. A. Coulson and A. Joseph, J. Quantum Chem. **1**, 337 [1967]. — H. A. Erikson and E. L. Hill, Phys. Rev. **75**, 29 [1949].

[36] K. Helfrich and H. Hartmann, Theor. Chim. Acta **24**, 271 [1972].

[37] M. E. Rose, Relativisttic Electron Theory, Wiley, New York 1961.

[38] A. S. Davydov, Quantenmechanik, Deutscher Verlag der Wissenschaften, Berlin 1967.

[39] R. B. McQuistan, Scalar and Vector Fields, Berliner Union, Stuttgart 1970.

[40] R. Courant and D. Hilbert, Methoden der Mathematischen Physik I, Kap. VII, Berlin 1968.

[41] B. Müller, J. Rafelski, and W. Greiner, Nuovo Cim. **18 A**, 551 [1973].

[42] M. E. Rose [37].

[43] I. Pomeranchuk and J. Smorodinsky, J. Phys. USSR **9**, 97 [1945].

[44] H.-J. Scheefer, Diplomarbeit, Frankfurt (Main) 1973.

[45] P. M. Morse and E. Stückelberg, Phys. Rev. **33**, 932 [1929].

[46] J. v. Neumann and E. Wigner, Z. Phys. **30**, 467 [1929].

[47] S. S. Gershtein and V. D. Krivchenkov, Exp. Theor. Phys. (USSR) **40**, 1491 [1961].

[48] A. S. Davydow, loc. cit. [38], p. 253.

[49] M. E. Rose, loc. cit. [37].

[50] A. S. Davydov, loc. cit. [38], p. 174 ff.

[51] W. Scheid, H. Müller, and W. Greiner, Phys. Rev. Lett. **32**, 741 [1974]; W. Scheid, J. Hofmann, and W. Greiner, Nuclear Shock Waves in Relativistic Heavy Ion Physics, Proc. of the Symposium on Physics with Relativistic Heavy Ions, Berkeley, July 1974.

[52] Calculations of this contribution are presently carried out by H. Peitz, Frankfurt (Main).

[53] F. Masnou-Seeuws, Transitions de Structure Fine par Collisions atome-atome et ion-atome, Thèse de Doctorat, Université Paris VII, 1973.

[54] K. Taulbjerg and J. Briggs have applied this method in a four-state calculation of K-vacancy sharing in asymmetric collisions. K. Taulbjerg private communication.

[55] J. Briggs and J. Macek, J. Phys. B **5**, 579 [1972]; see also W. Meyerhof, An Approximate Scaling Law for K-vacancy production in Symmetric Heavy Ion Collisions with $Z > 10$, preprint, Stanford 1974.

[56] F. C. Jundt, H. Kubo, and H. E. Gove, Phys. Rev. A **10**, 1053 [1974].

[57] D. Burch, W. B. Ingalls, H. Wieman, and R. Vandenbosch, Phys. Rev. A **10**, 1245 [1974].

[58] B. Müller, K. Smith, and W. Greiner, Spectroscopy of Superheavy Quasimolecules, preprint, Frankfurt (Main) 1974.

[59] a) W. Schäfer and G. Soff, Deviation from Rutherford Cross-section in Super heavy Quasi-Molecules, Nuovo Cim. in print. — b) J. Rafelski, Vacuum Polarization- and Molecular Potential Effects in Heavy Ion Scattering, preprint, Argonne 1974.

[60] R. K. Smith, Institut für Theoretische Physik der Universität Frankfurt (Main) 1974, private communication.

[61] N. Rosén, private communication.

[62] B. Fricke, K. Rashid, P. Bertoncini, and A. C. Wahl, Phys. Rev. Lett. **34**, 243 [1975].

[63] K. Rottmann, Mathematische Formelsammlung, Mannheim 1960.

[64] M. Abramowitz and I. Stegun, Handbook of Mathematical Functions, New York 1965.

[65] I. N. Sneddon, Spezielle Funktionen der Mathematischen Physik, Mannheim 1963.

[66] I. S. Gradshteyn and I. M. Ryzhik, Tables of Integrals, Series and Products, London 1961.

[67] A. H. Stroud and D. Secrest, Gaussian Quadrature Formulas, Englewood Cliffs 1966.

[68] R. Rabinowitz and G. Weiss, Math. Tables Aids Comp. **68**, 285 [1959].

[69] B. Müller, J. Rafelski, and W. Greiner, Phys. Lett. **47 b**, 5 [1973].